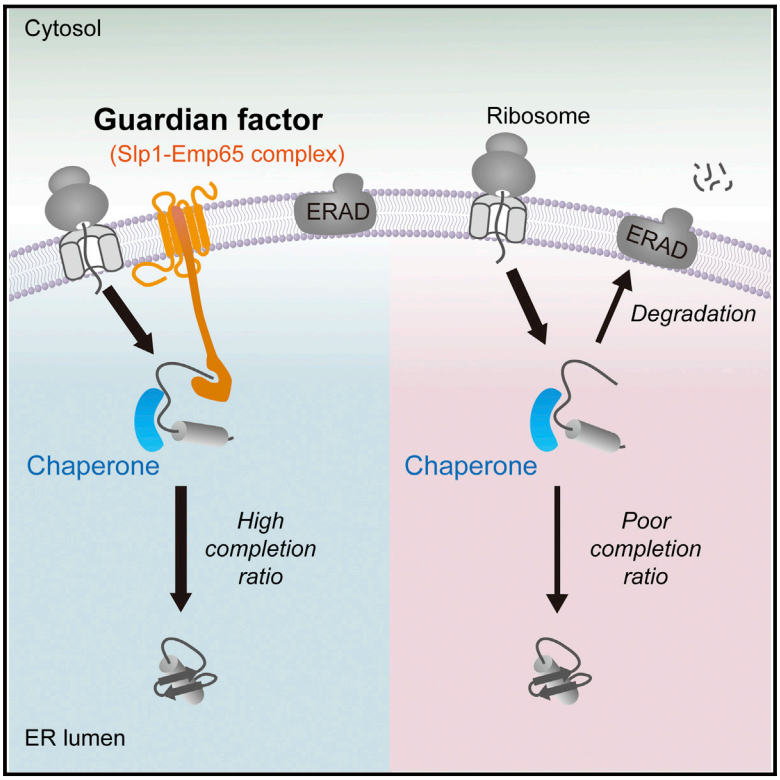
Article

Cell

Slp1-Emp65: A Guardian Factor that Protects Folding Polypeptides from Promiscuous Degradation

Graphical Abstract



Highlights

- Guardian factors protect actively folding polypeptides from degradation
- The Slp1-Emp65 complex represents the founding member of this class
- Protection is achieved through transient association of unfolded proteins
- In vivo validation of the glycan timer hypothesis of ER quality control

Authors

Shan Zhang, Chengchao Xu, Katherine E. Larrimore, Davis T.W. Ng

Correspondence

davisnglab@gmail.com

In Brief

A dedicated cellular mechanism protects folding polypeptides from degradation.

Zhang et al., 2017, Cell *171*, 1–12
October 5, 2017 © 2017 Elsevier Inc.
http://dx.doi.org/10.1016/j.cell.2017.08.036

CellPress

Please cite this article in press as: Zhang et al., Slp1-Emp65: A Guardian Factor that Protects Folding Polypeptides from Promiscuous Degradation, Cell (2017), http://dx.doi.org/10.1016/j.cell.2017.08.036

Article

Cell

Slp1-Emp65: A Guardian Factor that Protects Folding Polypeptides from Promiscuous Degradation

Shan Zhang,[1,2,4] Chengchao Xu,[1,2,4,5] Katherine E. Larrimore,[1] and Davis T.W. Ng[1,2,3,6,*]
[1]Temasek Life Sciences Laboratory
[2]Department of Biological Sciences
National University of Singapore, Singapore 117604, Singapore
[3]Duke-NUS Graduate Medical School, 8 College Road, Singapore 169857, Singapore
[4]These authors contributed equally
[5]Present address: Whitehead Institute for Biomedical Research, 455 Main St., Cambridge, MA 02142, USA
[6]Lead Contact
*Correspondence: davisnglab@gmail.com
http://dx.doi.org/10.1016/j.cell.2017.08.036

SUMMARY

Newly synthesized proteins engage molecular chaperones that assist folding. Their progress is monitored by quality control systems that target folding errors for degradation. Paradoxically, chaperones that promote folding also direct unfolded polypeptides for degradation. Hence, a mechanism was previously hypothesized that prevents the degradation of actively folding polypeptides. In this study, we show that a conserved endoplasmic reticulum (ER) membrane protein complex, consisting of Slp1 and Emp65 proteins, performs this function in the ER lumen. The complex binds unfolded proteins and protects them from degradation during folding. In its absence, approximately 20%–30% of newly synthesized proteins that could otherwise fold are degraded. Although the Slp1-Emp65 complex hosts a broad range of clients, it is specific for soluble proteins. Taken together, these studies demonstrate the vulnerability of newly translated, actively folding polypeptides and the discovery of a new proteostasis functional class we term "guardian" that protects them from degradation.

INTRODUCTION

Protein homeostasis or "proteostasis" describes the cellular processes that maintain and regulate the proteome. These activities include translation systems, protein trafficking and localization, protein folding and modification, and protein quality control and degradation. Through these mechanisms, proteins are placed in the correct concentrations and locations to form, establish, and sustain a cell. To maintain this level of control, the most intricate details are monitored by proteostasis regulatory networks (e.g., the heat shock and unfolded protein responses), which constantly make adjustments to ensure that balance is maintained (Balchin et al., 2016; Schneider and Bertolotti, 2015).

In the biosynthetic phase, translated products fold and assemble into their correct tertiary and quaternary structures. The efficiency of the process deceives the underlying complexity. An array of chaperones and modifying enzymes are used to produce simple monomers to large complexes containing multiple posttranslational modifications (Balchin et al., 2016). Errors can result in aberrant products that, unless neutralized, can be harmful and cause disease (Labbadia and Morimoto, 2015; Wang and Kaufman, 2016). Accordingly, sophisticated protein quality control systems are deployed to protect the cell against protein conformational toxicity. Although distinct pathways are found throughout the cell, those in the endoplasmic reticulum (ER), termed "ER quality control (ERQC)," are currently best understood (Cherepanova et al., 2016; Ruggiano et al., 2014; Xu and Ng, 2015).

Most proteins of the endomembrane system and those made for export are synthesized in the ER. This is a challenge for ERQC because of their structural and topological diversity coupled with a range of possible covalent protein modifications found nowhere else in the cell. ERQC must also retain actively folding and incompletely modified proteins because most maturation factors are ER-localized. Retaining harmful misfolded proteins is also important for their elimination by ER-associated degradation (ERAD) pathways. ERAD uses the ubiquitin-proteasome system (UPS), which is localized mostly outside the ER (Christianson and Ye, 2014; McCracken and Brodsky, 1996; Sommer and Jentsch, 1993; Ward et al., 1995). To engage the UPS, transmembrane complexes organized by ER/nuclear membrane E3 ubiquitin ligases (Hrd1, Doa10, and Asi1/3 in yeast) receive, translocate, and ubiquitinate substrates from ER membranes so the substrates can be degraded by 26S proteasomes (Carvalho et al., 2006; Foresti et al., 2014; Khmelinskii et al., 2014; Nakatsukasa et al., 2008; Vashist and Ng, 2004).

Chaperones play a crucial role for substrate recognition in ERAD (Araki and Nagata, 2011). In budding yeast, these include Kar2 (BiP), Scj1, Jem1, Lhs1, Pdi1, and Cne1 (Brodsky et al., 1999; Buck et al., 2013; Gillece et al., 1999; Kabani et al., 2003; Mehnert et al., 2015; Nishikawa et al., 2001; Silberstein et al., 1998). That these chaperones also play roles in protein folding raised a mechanistic quandary. How do folding

intermediates avoid degradation if they are bound to the same chaperones that are used in ERAD? An elegant hypothesis was formulated years earlier to address the conundrum (Helenius and Aebi, 2004). It posited that degradation is delayed by a mechanism to provide time for folding. Proteins that remain unfolded beyond the window are then targeted for degradation. The proposed mechanism for the folding "timer" was sequential N-glycan trimming of glucosyl and mannosyl residues, a conserved activity whose physiological role was not fully clear (Helenius and Aebi, 2001). The idea was supported by the discovery of an integrated system that features the α-mannosidase Htm1 (the EDEM family in metazoans) and lectin-like receptor Yos9 (OS-9 and XTP-3B in mammals) (Bhamidipati et al., 2005; Buschhorn et al., 2004; Christianson et al., 2008; Kim et al., 2005; Molinari et al., 2003; Oda et al., 2003; Szathmary et al., 2005). Htm1, through its association with protein disulfide isomerase, targets unfolded proteins bearing $Man_8GlcNAc_2$ glycans and cleaves a single mannose residue from the C-arm (Gauss et al., 2011; Pfeiffer et al., 2016). This event exposes a terminal α1,6-linked mannosyl residue, the ligand for Yos9 that initiates ERAD of the substrate (Quan et al., 2008). Unexpectedly, cells engineered to bypass the trimming delay by directly appending an ERAD glycan signal during synthesis did not increase substrate degradation rates (Clerc et al., 2009). Thus, the finding hinted at a distinct and perhaps more universal mechanism that protects actively folding proteins from degradation, especially as not all proteins synthesized in the ER are glycosylated.

For non-glycosylated luminal proteins, glycan-independent mechanisms exist. One is dependent on the Hrd1 complex but can function independently of glycan-dependent components (Kanehara et al., 2010; Okuda-Shimizu and Hendershot, 2007). The other, characterized by the ΔGppαF model substrate (non-glycosylated form of pro-α-factor), uses the UPS, but its specific E3 ubiquitin ligase remains unknown (Werner et al., 1996). For unglycosylated proteins, no mechanism is known that prevents their degradation during folding.

In this study, we report the conserved ER Slp1-Emp65 complex as a guardian factor that protects newly synthesized, folding polypeptides from degradation. The discovery of this activity revealed an intrinsic vulnerability of maturing polypeptides to ER degradation systems. Our data show that this previously unknown component of the proteostasis machinery promotes the integration of protein folding and ERQC, processes that share many common effectors but have opposing outcomes. The inclusion of this mechanism as part of cellular protein homeostasis makes an aggressive quality control system compatible with a folding platform requiring a high degree of efficiency.

RESULTS

SLP1 and *EMP65* Are Identified through a Genetic Screen for Mutants of ER Dysfunction

GFP poorly folds in the ER of yeast and of mammalian cells (Aronson et al., 2011; Xu et al., 2013). In yeast, this deficiency can be overcome by expressing a fast-folding variant called "ER-GFP^{fast}" (Fisher and DeLisa, 2008; Xu et al., 2013). ER-GFP^{fast} was designed for a different purpose, but we recognized that it could report on the folding environment of the ER. To test this idea, we expressed ER-GFP^{fast} in a haploid yeast gene knockout subset, each displaying the phenotype of constitutive ER stress activation (Jonikas et al., 2009). Of 236 strains, 27 strains displayed a reduction of fluorescence activity (normalized for protein level) of 20% or greater (Table S1). Although a few genes directly involved in protein folding were identified (*SIL1*, *CNE1*, and *SCJ1*), the remaining have functions as diverse as glycosylation, lipid metabolism, protein trafficking, and chromatin remodeling. Because ER-GFP^{fast} is an extensively engineered foreign protein, we surmised that its folding is sensitive to diverse forms of ER perturbations, making it a useful tool to study broad aspects of ER homeostasis. Of the genes identified, we chose to focus on the *SLP1* and *EMP65* genes because they encode a highly conserved ER transmembrane protein complex whose molecular function is unknown (Figures 1A and S1A–S1C) (Friederichs et al., 2012; Hein et al., 2015).

To determine a role for the Slp1-Emp65 complex (hereby termed S-E complex for simplicity), we generated strains lacking each gene in the W303 background (Figure 1B). First, we analyzed the biosynthesis of Gas1, a glycosylphosphatidylinositol (GPI)-anchored plasma membrane protein in wild-type (WT) and mutant strains. Gas1 is ideal for this purpose because its maturation includes N-linked glycosylation, *O*-mannosylation, intramolecular disulfide bonds, and a GPI anchor (Nuoffer et al., 1991). In addition, its translocation into the ER is through the Sec61/62/63 complex and folding failures are retained in the ER and subject to ERAD (Fujita et al., 2006; Ng and Walter, 1996). Only correctly folded and modified Gas1 can exit the ER, where its glycans are extended in the Golgi apparatus (Hirayama et al., 2008). Defects in any of these activities can be detected quantitatively by metabolic pulse-chase/immunoprecipitation assay (PC/IPA) (Ng and Walter, 1996). As shown in Figure 1C, Gas1 processing in *slp1* and *emp65* knockout strains is identical to WT indicating that ER protein biosynthetic activities including translocation, glycosylation, oxidation, folding, and trafficking are not generally perturbed. We obtained the same result in the *slp1emp65* double-knockout strain, ruling out functional redundancy between the genes (Figure S1D). It was previously reported that loss of either gene causes activation of the unfolded protein response (UPR) (Jonikas et al., 2009). To measure the extent of activation in our own strains, *slp1* and *emp65* knockout cells were transformed with a β-galactosidase gene reporter specifically responsive to ER stress (Cox and Walter, 1996). Compared to WT cells, *Δslp1* and *Δemp65* cells displayed modest and reproducible induction of approximately 2-fold, indicating some form of ER dysfunction not revealed by Gas1 maturation (Figures 1C and 1D). Importantly, their treatment with the glycosylation inhibitor tunicamycin induced the UPR similar to WT confirming that their ER stress response is not impaired (Figure 1D).

The S-E Complex Prevents the Erroneous Degradation of Unfolded Proteins

As *SLP1* and *EMP65* are not required generally for protein biosynthesis, we analyzed the state of ER protein quality control in mutants lacking the genes. For this purpose, the degradation of two classical soluble ERAD substrates, CPY* and PrA*, was measured by PC/IPA (Finger et al., 1993). Both proteins

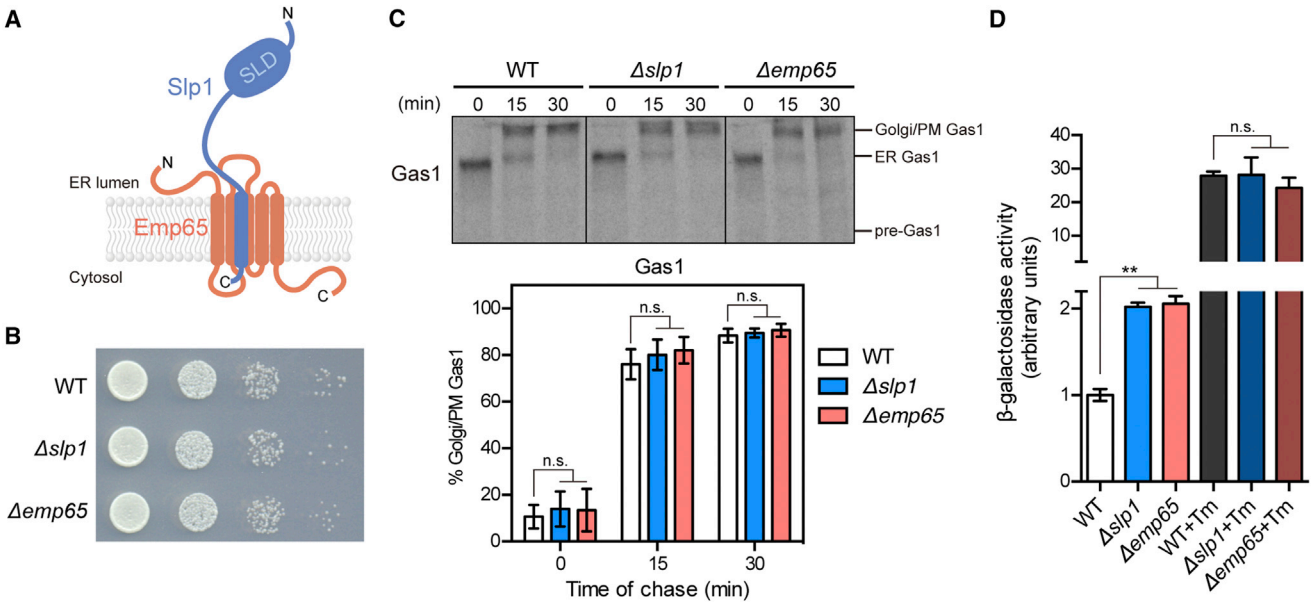


Figure 1. Major ER Functions Are Unimpaired in *SLP1* and *EMP65* Mutants

(A) Schematic representation of the Slp1-Emp65 complex (Sohaskey et al., 2010).

(B) Serial dilutions of WT, *Δslp1*, and *Δemp65* cells were spotted and incubated at 30°C.

(C) Cells were pulse-labeled for 5 min with [^{35}S]Met/Cys, followed by the addition of cold Met/Cys and chased for the times indicated. Endogenous Gas1 was immunoprecipitated, separated by SDS-PAGE, and visualized/quantified by phosphorimager analysis. Representative gel images are shown. Untranslocated Gas1 (pre-Gas1), ER (ER Gas1), and Golgi/ plasma membrane (Golgi/PM Gas1) forms are indicated (upper panel) and quantified (lower panel). The data represent ± SEM of three independent experiments. Student's t test: $p \geq 0.05$, n.s., not significant, *$p < 0.05$, **$p < 0.01$, and ***$p < 0.001$.

(D) UPR activity in *Δslp1* and *Δemp65* cells was measured by a β-galactosidase reporter assay. Cells were untreated or incubated with 2.5 μg/mL of tunicamycin (Tm) for 1 hr. UPR activity is plotted as arbitrary units with the activity of untreated WT cells set to 1.0.

Data represent mean ± SEM. See also Figure S1 and Table S1.

degraded rapidly in WT cells as expected (Figures 2A and 2B). A degradation delay, consistent with a role in ERAD, was not observed in mutant cells. Instead, substrate degradation was aberrantly enhanced. To extend the range of substrates, we expressed the non-glycosylated form of pro-α-factor called "ΔGppαF." The ERAD pathway that acts on ΔGppαF is somewhat enigmatic because the E3 ligase is unidentified (McCracken and Brodsky, 1996; Werner et al., 1996). As shown in Figure 2C, ΔGppαF is efficiently degraded in WT cells and even more rapidly degraded in *Δemp65* and *Δslp1* cells. These data show that the S-E complex can also act on non-glycosylated proteins. The observed effects occurred immediately after the pulse, suggesting the loss of S-E complex function caused a more aggressive degradative attack on newly synthesized unfolded proteins. To explore this notion, we expressed a variant of CPY* in cells lacking the S-E complex (Xie et al., 2009). The variant, called "abcd-CPY*," lacks all four N-glycans, and despite being misfolded and retained in the ER, poorly degrades even in WT cells because it cannot generate the ERAD glycan signal (Figure S2A) (Quan et al., 2008; Xie et al., 2009). Remarkably, abcd-CPY* is degraded in *slp1* and *emp65* cells. These data show that the S-E complex broadly restrains the degradation of newly synthesized unfolded proteins in the ER.

Next, we assessed which of the known degradation pathways for misfolded proteins provides the enhancement. CPY* is degraded by ERAD under normal conditions and trafficked to vacuole for degradation under stress (Spear and Ng, 2003). Here, we generated double-mutant strains lacking *SLP1* combined with *UBC7*, *CDC48* (genes required for all known ERAD pathways), or *PEP4* (activation of vacuolar proteases) (Ammerer et al., 1986; Foresti et al., 2014). In Δ*ubc7* and *cdc48-1* single mutants, CPY* is strongly stabilized compared to WT as expected (Figure 2D, left panel, and S2B). The *ubc7slp1* and *cdc48-1slp1* double mutants eliminated or strongly inhibited enhanced degradation showing that the effect is dependent on ERAD (Figure 2D, right panel, and S2B). By contrast, deleting *PEP4* did not alter CPY* degradation in the *slp1* background, indicating vacuolar proteases do not contribute (Figure S2C). Because CPY* (and PrA*) degradation is glycan-dependent, we tested whether accelerated ERAD relies on Htm1 (ERAD mannosidase) and Yos9 (ERAD lectin receptor) (Clerc et al., 2009; Knop et al., 1996). Enhanced degradation was observed in *htm1slp1* and *yos9slp1* strains but the effect is somewhat diminished suggesting protection from both glycan-dependent and glycan-independent pathways (Figure S2D). Because ERAD pathways are sometimes defined by their specific E3 ubiquitin ligases, we deleted the known ligase genes with effect on ERAD. The *HRD1* (ERAD-L*uminal* and ERAD-M*embrane*) and *DOA10* (ERAD-C*ytosolic*) genes play roles degrading most model ERAD substrates in budding yeast (Carvalho et al., 2006; Vashist and Ng, 2004). The loss of either gene did not fully disrupt enhanced degradation of CPY* but smaller effects are difficult

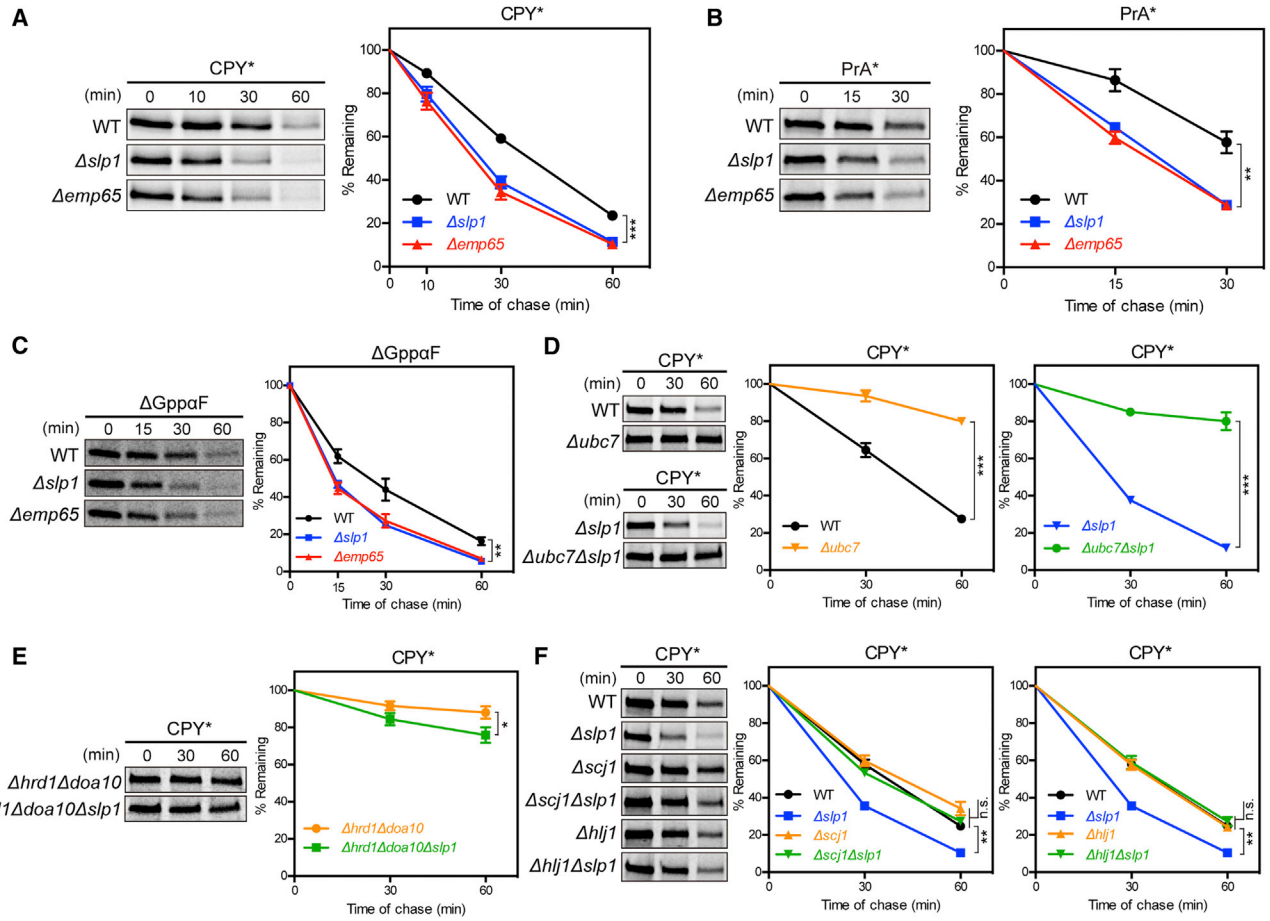


Figure 2. Dysregulated ERAD in *SLP1* and *EMP65* Mutants

(A) WT, *Δslp1*, and *Δemp65* cells expressing HA-epitope-tagged CPY* were pulse-labeled with [^{35}S]Met/Cys for 10 min and chased for the times indicated. CPY* was immunoprecipitated and resolved by SDS-PAGE. Data from three independent experiments were quantified by phosphorimager analysis and plotted as ± SEM.

(B) Turnover of PrA* performed like in (A), except with a 5 min pulse-label.

(C) ΔGppαF turnover analyzed like in (A).

(D) CPY* degradation in WT, *Δubc7*, *Δslp1*, and *Δubc7Δslp1* cells was analyzed like in (A).

(E) CPY* stability in *Δhrd1Δdoa10* and *Δhrd1Δdoa10Δslp1* cells was analyzed like in (A).

(F) CPY* turnover was analyzed in WT, *Δslp1*, *Δscj1*, *Δscj1Δslp1*, *Δhlj1*, and *Δhlj1Δslp1* cells as described in (A).

In (B)–(F), data represent mean ± SEM. See also Figure S2.

to discern and the two factors sometimes display substrate overlaps (Figure S2E) (Gnann et al., 2004). Knocking out both genes in the *Δslp1* background strongly reduced enhanced degradation indicating these E3 enzymes play a significant role (Figure 2E). However, the effect was not abolished suggesting the contribution of other E3 enzymes. Other quality control E3 ligase genes, including *ASI1* (inner-nuclear membrane quality control) (Foresti et al., 2014; Khmelinskii et al., 2014), *SAN1*, and *UBR1* (nuclear and cytosolic quality control) (Gardner et al., 2005; Heck et al., 2010; Prasad et al., 2010; Stolz et al., 2013), did not disrupt dysregulated degradation (Figure S2F).

ERAD substrates require chaperones for degradation. To extend our analysis, we tested the ER J class chaperones Scj1 and Hlj1, both with roles in ERAD (Nishikawa et al., 2001; Youker et al., 2004). In *scj1* and *hlj1* single mutants, there was little effect on CPY* degradation under non-stress conditions as previously reported (Figure 2F) (Nishikawa et al., 2001). However, combined with the *slp1* background, accelerated degradation was completely blocked. Taken together, these data show that the S-E complex functions to temporarily prevent the degradation of unfolded proteins of multiple ERAD pathways.

The S-E Complex Protects Normal Proteins from Promiscuous Degradation

Physiologically, what is the purpose of restraining ERAD? For the model ERAD substrates examined, the answer is not obvious because they can never fold so faster elimination seems favorable. However, for normal proteins, this function could be critical. The S-E complex might provide a timer function that shields folding polypeptides from degradation as previously proposed

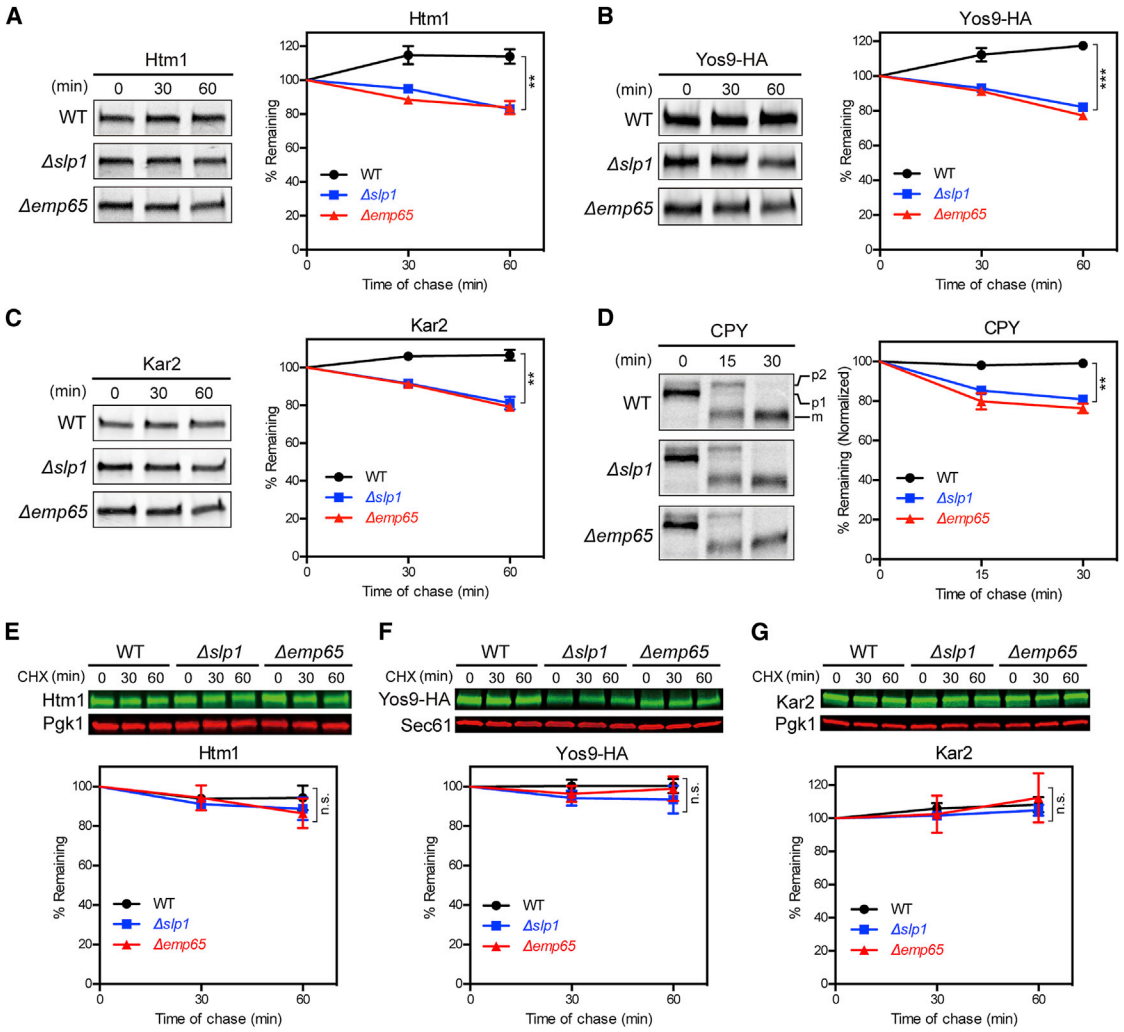


Figure 3. The S-E Complex Prevents Degradation of Folding Polypeptides

(A–D) WT, *Δslp1*, and *Δemp65* cells were pulse-labeled for 10 min (Htm1, Yos9-HA, and Kar2) or 5 min (CPY) and chased for the times indicated. Proteins were immunoprecipitated using protein-specific antibodies; anti-Htm1 antibody in (A), anti-HA antibody in (B), anti-Kar2 antibody in (C), and anti-CPY antibody in D. Proteins were separated by SDS-PAGE and analyzed as described in Figure 2A. In (D), quantification of CPY was normalized to compensate for the loss of labeled amino acids in the "pro" domain after vacuolar processing. p1 (ER), p2 (Golgi), and m (vacuolar) forms of CPY are indicated. Data represent mean ± SEM. (E–G) WT, *Δslp1*, and *Δemp65* cells were treated with 200 μg/mL of cycloheximide to terminate translation for the times indicated. Cell extracts were separated by SDS-PAGE, and proteins were analyzed by quantitative immunoblotting using specific antibodies. Pgk1 was probed to control for loading in (E) and (G). Sec61 was probed to control for loading in (F). Data represent mean ± SEM.

See also Figures S3 and S4.

(Helenius and Aebi, 2004). To test this idea directly, we analyzed the fate of normal proteins during their folding and maturation by PC/IPA. For this purpose, we examined the ER resident proteins Htm1, Yos9, Kar2, and the vacuolar protein CPY. In WT cells, these newly synthesized proteins are stable over 60 min reflecting efficient folding, typical of most yeast proteins (Figures 3A–3D; WT) (Duttler et al., 2013). By contrast, the same proteins in mutant cells displayed overall degradation of 20%–30% during the time course that started immediately after the chase (Figures 3A–3D; *Δslp1* and *Δemp65*). This effect is not a result of strain background because the same result was obtained in BY4742 cells (Figures S3A–S3C). The ER-GFP^{fast} reporter also displays dysregulated degradation in *Δslp1* and *Δemp65* cells (Figures S3D and S3E). This result shows that the S-E complex performs a basic biochemical function that is not restricted to endogenous proteins. Although these data are consistent with a protective function for unfolded proteins, it is also possible that loss of Slp1-Emp65 causes indiscriminate degradation of ER proteins. To address this possibility, we performed cycloheximide chase experiments to analyze the fate of folded proteins. Unlike the PC/IPA experiments, which follow the fate of newly made proteins, cycloheximide chase experiments examine the fate of pre-existing proteins. For normal long-lived proteins, the steady-state population is essentially fully folded because

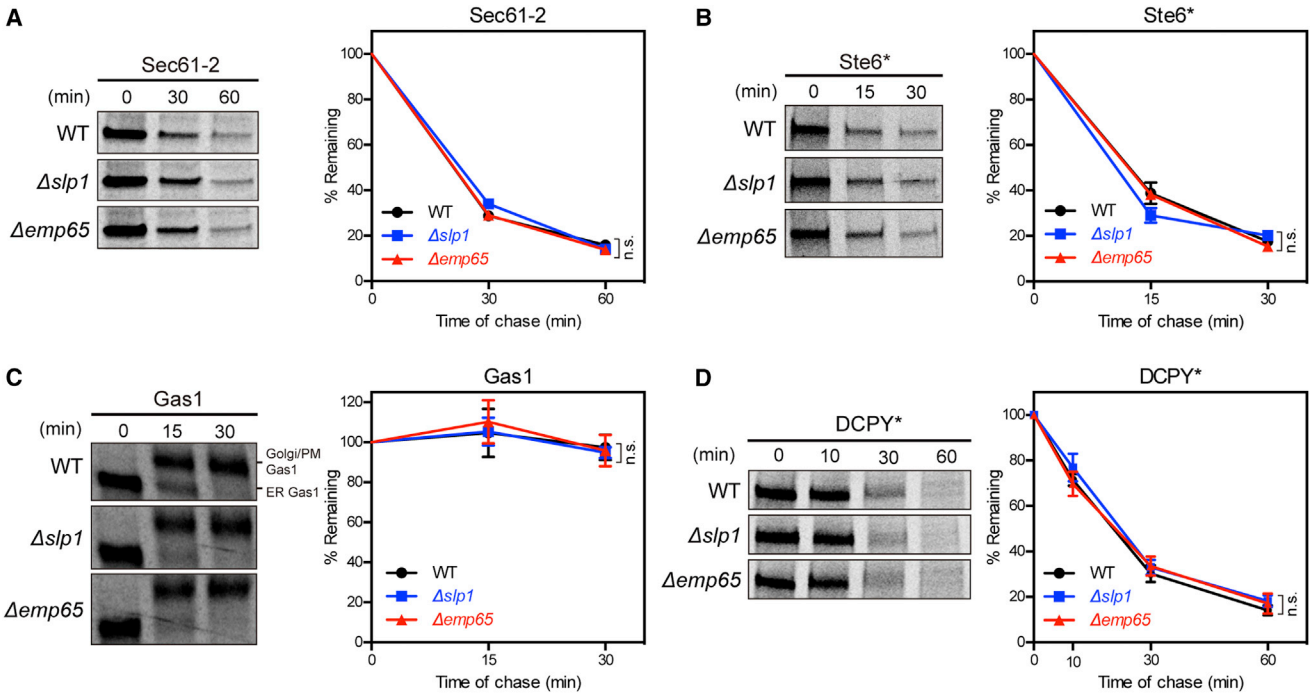


Figure 4. Membrane Proteins Are Not Clients of the S-E Complex

(A) Stability of the integral membrane ERAD substrates Sec61-2 (ERAD-M) was analyzed by PC/IPA as described in Figure 2A.

(B) Turnover of ERAD substrates Ste6* (ERAD-C) was analyzed by PC/IPA as described in Figure 2A, except the pulse-labeling time was 5 min.

(C) Stability of endogenous GPI-anchored protein Gas1. The data were quantified from the experiments shown in Figure 1C. Here, all forms of Gas1 were summed for each plotted time point.

(D) Stability of DCPY* (ERAD-L) were analyzed by PC/IPA as described in Figure 2A.

Data represent mean ± SEM. See also Figures S5 and S6.

unfolded molecules represent a minor population and misfolded proteins are rapidly degraded. Here, the ER resident proteins Htm1, Yos9, and Kar2 were equally stable in WT and mutant strains showing that the folded population is not subject to degradation (Figures 3E–3G). By contrast, applying the same experiment to CPY* and PrA*, their degradation is efficient in all strains (again, faster in mutant strains). This result demonstrates that ERAD's ability to recognize and degrade misfolded proteins is not impaired when lacking Slp1-Emp65 (Figure S4). These data show that Slp1-Emp65 is specifically required to prevent erroneous degradation of actively folding proteins. We propose the term "guardian" to describe the activity.

The Guardian Activity of Slp1-Emp65 Is Specific to Soluble Proteins in the ER Lumen

All clients of the S-E complex determined so far are soluble proteins. To assess whether the client range includes membrane proteins, we tested ERAD substrates Sec61-2 (ERAD-M) and Ste6* (ERAD-C). Both proteins were degraded with the same kinetics in WT and mutant cells indicating that they are not clients of the S-E complex (Figures 4A and 4B). For normal proteins, we quantified total Gas1 in the experiment shown in Figure 1C to determine its stability. Like other membrane proteins examined, Gas1 is stable in *slp1* and *emp65* mutants (Figure 4C). To understand what determinants identify an S-E complex client, we anchored CPY* to the ER membrane by replacing its signal sequence with the N-terminal signal anchor domain of DPAP B as designed by the Stirling lab previously (Willer et al., 2008). The previous study showed that the chimera, although anchored in the membrane, used the same ERAD-L pathway as soluble CPY* (Figure S5). Here, while DCPY* is rapidly degraded in control cells as expected, its degradation rate was unchanged in *slp1* and *emp65* mutants compared to WT (Figure 4D). Thus, for DCPY*, despite displaying all the determinants of soluble CPY*, the S-E complex does not invoke a degradation delay. These data demonstrate that, unlike ERAD pathways, S-E complex clients are primarily soluble proteins in the ER lumen.

The S-E Complex Binds Unfolded Polypeptides Transiently

The data show that the S-E complex protects nascent polypeptides from degradation so full folding efficiency is achievable. It doesn't regulate the ERAD machinery otherwise CPY* and DCPY*, substrates of glycan-dependent ERAD-L, would be equally affected in *slp1* and *emp65* mutants. Alternatively, the S-E complex might engage its clients directly to regulate their accessibility to ERAD. To address this question, we performed native co-immunoprecipitation (coIP) assays in cells expressing fully functional HA epitope-tagged Slp1, which contains a large luminal domain (Figures 1A and S6). Because any interaction is expected to be transient, starting material was greater than typical for coIP assays (see the Method Details). The assay was applied

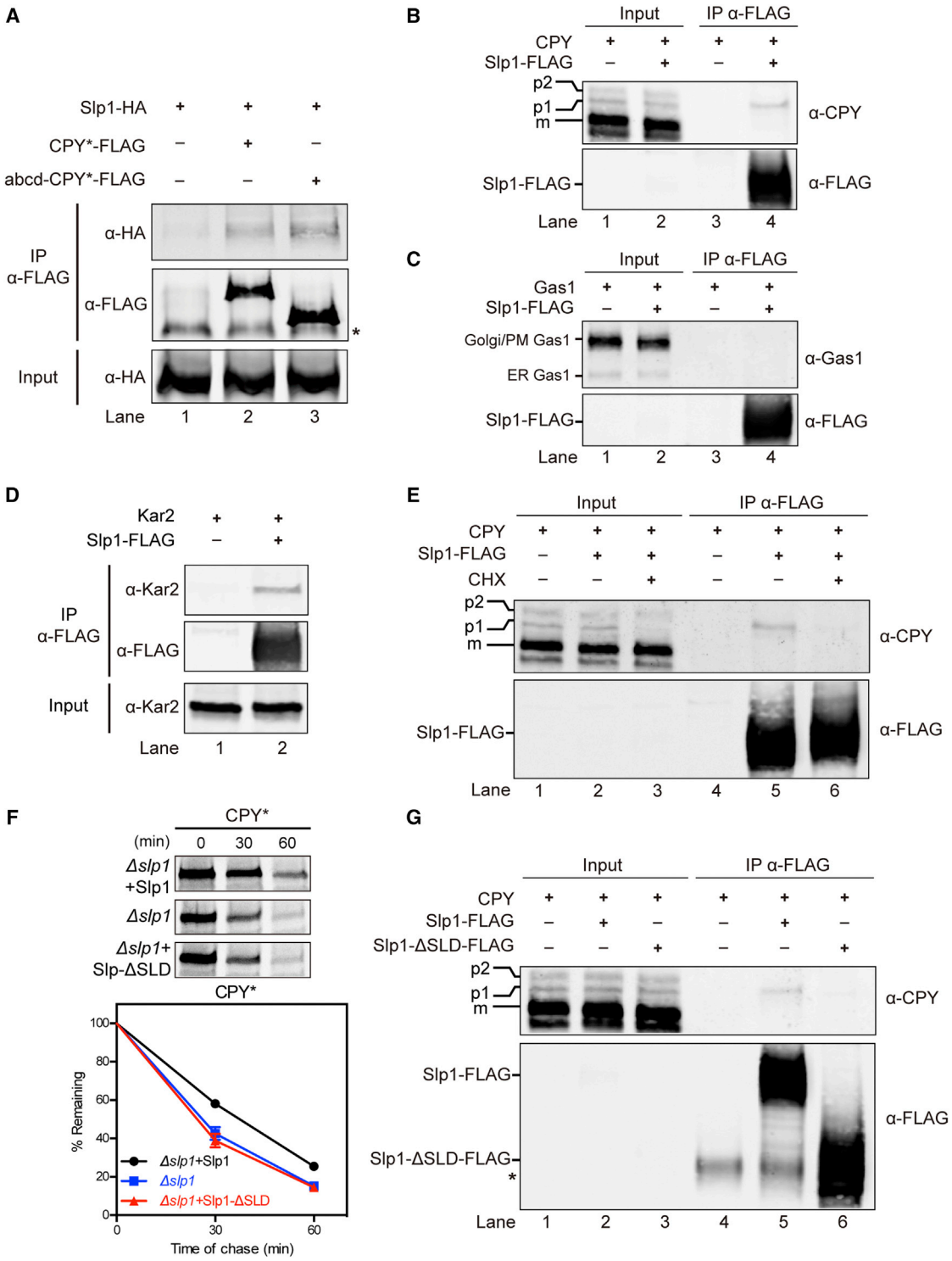


Figure 5. Slp1 Specifically Binds to Unfolded Soluble Proteins in the ER

(A) Extracts prepared from the indicated cells co-expressing Slp1-HA and CPY*-FLAG or abcd-CPY*-FLAG were incubated with anti-FLAG antibody resin. Bound proteins were eluted using triple-FLAG peptide, resolved by SDS-PAGE, and visualized by immunoblotting. The asterisk denotes a non-specific signal.

(B–D) Extracts prepared from the indicated cells expressing Slp1-FLAG were processed as described in (A). Eluted proteins were analyzed by immunoblotting with anti-FLAG and anti-CPY antibodies in (B), anti-FLAG and anti-Gas1 antibodies in (C), and anti-FLAG and anti-Kar2 antibodies in (D).

(legend continued on next page)

to CPY* and abcd-CPY* and separately co-expressed with Slp1-HA. Both unfolded proteins were associated with Slp1 (Figure 5A). Next, we examined the endogenous protein CPY in cells expressing functional Slp1-FLAG. The ER (p1), Golgi (p2), and vacuolar forms (mCPY) of CPY are clearly distinguished by gel mobility (Figure 5B). Importantly, Slp1-FLAG associates exclusively with the ER form of proCPY even though that represents but a small fraction of total CPY at steady state (Figure 5B, lane 4). By contrast, an interaction between Slp1 and the GPI-anchored protein Gas1 was not detected in the same experiment (Figure 5C). In addition, an interaction between Slp1-FLAG and Kar2 was detected (Figure 5D). It should be noted that although Kar2 is a client, it's possible that some association is through its role as a folding chaperone (i.e., folded Kar2 is bound to unfolded S-E complex clients). Next, we examined the nature of the Slp1-client interaction. First, we repeated the experiment described in Figure 5B, but with the added step of a cycloheximide chase to determine the stability of the interaction. In the absence of cycloheximide, p1 CPY is associated with Slp1 (Figure 5E, lane 5). This interaction is completely abolished after a short chase demonstrating the interaction is transient (Figure 5E, lane 6). Slp1 contains a Sad1-UNC84 homology domain (SUN-like domain) on its luminal side. This is homologous to the SUN domain of the SUN protein family that is known to bind peptide ligands (Sosa et al., 2012). To determine the importance of the SUN-like domain in Slp1-client interactions, an Slp1 variant (Slp1-ΔSLD) lacking it was constructed. Slp1-ΔSLD failed to complement dysregulated degradation in a *Δslp1* strain (Figure 5F) showing that it is not functional in this role. In coIP experiments, while Slp1-FLAG specifically bound the ER form of endogenous proCPY, Slp1-ΔSLD-FLAG did not associate with any form of CPY (Figure 5G, compare lanes 5 and 6). Note that the steady state level of Slp1-ΔSLD-FLAG is similar to Slp1-FLAG, suggesting that it is not grossly misfolded (Figures 5G and S7D, lower panel). Together, these data support a mechanism by which the S-E complex protects newly synthesized proteins from ERAD through binding and release. In the absence of either component or the SUN-like domain of Slp1, the absence of engagement with the complex makes unfolded protein susceptible to degradation.

Guardian Activity Functions in Parallel with the Glycan Timer for Glycosylated Clients

The data indicate that the S-E complex protects newly synthesized proteins against degradation during the folding process. Thus, the S-E complex seems to perform the role proposed for the glycan timer mechanism of ER quality control (Helenius and Aebi, 2004). However, *alg3* mutants, which bypass the trimming delay by appending the glycan degradation signal during synthesis, did not change the rate of degradation as could be predicted (Clerc et al., 2009). From our current understanding, we reasoned that the expected accelerated CPY* degradation, by glycan-dependent ERAD, was prevented by the activity of S-E complex. To test this idea directly, we measured CPY* degradation in *Δalg3Δslp1* cells. Here, CPY* degraded even more rapidly than in *Δslp1* cells alone (Figure 6A, right). The further enhancement of accelerated degradation is via glycan-dependent ERAD because abcd-CPY* displayed no change (Figure 6B). These data show that the S-E complex can protect substrates from glycan-dependent ERAD should they display the glycan signal prematurely. Interestingly, these experiments reveal the time delay imposed by the glycan timer, an effect previously masked by the more universal guardian activity.

DISCUSSION

The genes encoding the Slp1-Emp65 complex are evolutionary conserved among all eukaryotes analyzed and make up a distinct subfamily of SUN domain family (Vasnier et al., 2014). In mammals, the Slp1 and Emp65 homologs are called SUCO (or OPT) and TAPT1, respectively. As in yeast, they form an ER membrane protein complex (Friederichs et al., 2012). In plants and mammals, S-E complex homologs are ubiquitous, being expressed in all tissues tested (Howell et al., 2007; Li et al., 2011; Sohaskey et al., 2010). The universality of the S-E complex is a strong indicator that it plays a common, critical role in all eukaryotic cells. Indeed, the diversity of phenotypes observed in different systems, seemingly unrelated, actually supports the view of a basic fundamental function (Howell et al., 2007; Li et al., 2011; Sohaskey et al., 2010).

The assorted phenotypes of S-E complex mutants can be attributed to the guardian activity described here. In budding yeast, loss of the S-E complex results in the leakage of the ER resident Kar2 into the secretory pathway (Copic et al., 2009). In the genome-wide screen for mutants that secrete Kar2, 87 gene deletion strains were identified. These mutants represent diverse ER functions including glycosylation, GPI anchorage, protein retrieval, and protein quality control so the guardian activity of the S-E complex falls well within this group (Copic et al., 2009). In the filamentous fungus *Sordaria macrospora*, *SLP1* mutants display a karyogamy (nuclear membrane fusion) defect (Vasnier et al., 2014). Similarly, mutations in Kar2, Sec63, Sec71, and Sec72, proteins involved in early ER protein biogenesis and quality control, all cause karyogamy defects in budding yeast (Ng and Walter, 1996; Rose et al., 1989). In *Arabidopsis thaliana*, mutants of the Emp65 homolog POD1 are defective in pollen tube guidance (Li et al., 2011). How the S-E complex

(E) The indicated cells expressing Slp1-FLAG were incubated in the presence or absence of 200 μg/mL cycloheximide for 15 min. Extracts were prepared as described in (A), with anti-FLAG and anti-CPY antibodies used in immunoblotting.

(F) CPY* degradation in *Δslp1* cells carrying vectors expressing WT Slp1, Slp1 lacking SUN-like domain (Slp1-ΔSLD), or empty vector was analyzed by PC/IPA as described in Figure 2A. Data represent mean ± SEM.

(G) Extracts prepared from cells expressing FLAG-epitope-tagged Slp1 or Slp1-ΔSLD were processed as described in (A). The asterisk denotes the position of a non-specific signal. 5% of the total lysates were loaded as input in panels A and D. 1% of the total lysates were loaded as input in (B), (C), (E), and (G) to better detect isoforms of CPY and Gas1. FLAG-tagged proteins are not visualized here. See Figure S7 to visualize Slp1-FLAG and Slp1-ΔSLD-FLAG (5% of total input loaded).

See also Figure S7.

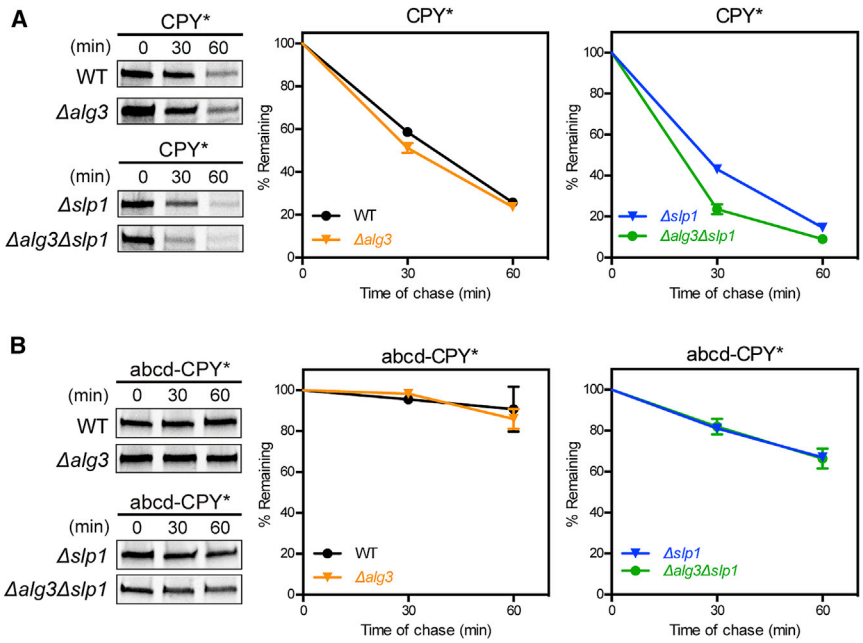


Figure 6. The S-E Complex Protects against Premature Degradation by Glycan-Dependent ERAD

(A) CPY* degradation in WT, *Δalg3*, *Δslp1*, and *Δalg3Δslp1* cells was analyzed like in Figure 2A.

(B) Turnover of abcd-CPY* in WT, *Δalg3*, *Δslp1*, and *Δalg3Δslp1* cells was analyzed as described in Figure 2A.

Data represent mean ± SEM.

affects this aspect of plant development is less clear because the process is complex (Li et al., 2011). Nevertheless, the process would involve signaling molecules and cellular remodeling, activities normally reliant on the ER. Of all reported phenotypes, the loss of the mouse *SLP1* homolog *Opt* is the most intriguing because the major phenotype is likely the direct consequence of guardian activity loss. $Opt^{-/-}$ mice display severe bone abnormalities caused by a dramatic reduction of type I collagen (Sohaskey et al., 2010). Type I collagen biosynthesis begins in the ER where the individual chains undergo extensive prolyl hydroxylation to fold and assemble into extended triple helical chains (Boudko et al., 2012). Like the S-E complex clients in yeast, intracellular collagens are soluble proteins. In $Opt^{-/-}$ mice, collagen mRNA levels are normal so the protein loss is caused by either a reduced translation or abnormal degradation, an issue not yet addressed (Sohaskey et al., 2010). Poor translation is unlikely because most proteins are normal in $Opt^{-/-}$ mice and we've not observed translational defects in our PC/IPA experiments. Based on the findings here, we predict that the $Opt^{-/-}$ phenotype reflects abnormal degradation of Type I collagen. The unusual nature of collagen biogenesis could make it particularly dependent on guardian activity of the S-E complex, making it more susceptible to loss than other clients.

The data presented here for the S-E complex satisfy the requirements of a folding timer generally hypothesized by Helenius and Aebi (2004), but we favor a simpler view. We propose that the S-E complex temporarily isolates vulnerable nascent proteins from ERAD so they can fold. Our data indicate that the mechanism is through client molecule binding and release. This association is specific because only bona fide client molecules are detected associated with the complex (Figure 5). Consistent with the proposed mechanism, structural insights from the canonical SUN domain suggest that the SUN-like domain of Slp1 is ideally suited for this function. The SUN-like domain of Slp1 shares overall 33% sequence similarity to the SUN domain of the mammalian SUN2, suggesting a degree of structural similarity. SUN proteins form a molecular tether that connects the outer nuclear membrane to the inner nuclear membrane. X-ray crystallographic analysis of mammalian SUN2 revealed that the SUN domain ligand is an unstructured, extended peptide of KASH (Klarsicht, ANC-1, and Syne homology) domain proteins, a structure commonly found in unfolded proteins (Sosa et al., 2012). Combining structural information with our data (Figure 5), we propose that the SUN-like domain of Slp1 binds extended segments of unfolded proteins directly but with relaxed sequence specificity to accommodate the broad range of substrates observed.

The discovery of the S-E complex as a guardian factor fills significant gaps in our understanding of ER quality control. Foremost, the S-E complex functions to protect folding proteins, glycosylated and non-glycosylated, from degradation. As importantly, its discovery revealed that newly synthesized proteins are particularly prone to degradation, perhaps by transiently displaying degrons that disappear as secondary and tertiary structures form. This dynamic is seen most clearly with abcd-CPY*, which is stable in WT cells yet partially degraded in *Δslp1* and *Δemp65* cells (Figure S2A). Its stability is due to its inability to form its glycan ERAD signal after folding attempts. Without guardian activity, abcd-CPY* is degraded in a short time window after synthesis because little of the accumulated steady-state population is subject to degradation (our unpublished results). Interestingly, an important and appealing side product of our study is the in vivo validation of the mannose timer hypothesis for protein folding (Helenius and Aebi, 2004). By eliminating the general delay imposed by the S-E complex, the effect of bypassing the sequential glycan trimming steps in *Δalg3* cells could be observed clearly (Figure 6A). Thus, the enigma of why directly appending the glycan ERAD signal during synthesis failed to increase degradation rates could be solved (Clerc et al., 2009).

The S-E complex is not required for viability in yeast but its presence increases the efficiency of producing functional proteins from 70%–80% (perhaps even lower for some proteins like Type I collagen) to nearly 100%, certainly the more favorable circumstance. In mammals, the S-E complex is essential because $Opt^{-/-}$ mice are neonatal lethal (Sohaskey et al., 2010). Although the presence of the S-E complex dramatically impacts the productive synthesis of proteins, it does not function

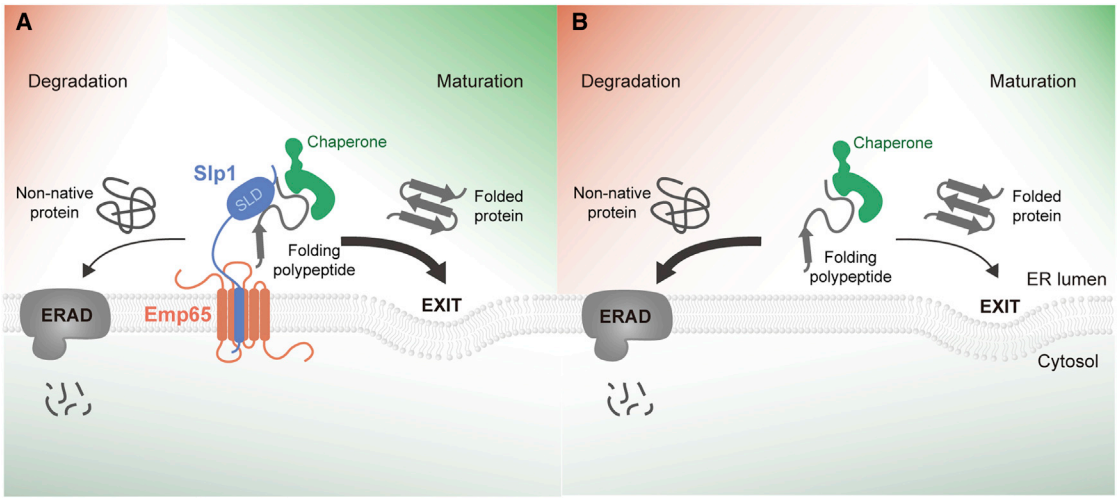


Figure 7. Proposed Mechanism of the Slp1-Emp65 Guardian Factor

(A) Newly synthesized soluble proteins are translocated into the ER lumen and engage chaperones for folding. Association of folding intermediates with the Slp1-Emp65 complex prevents their entry into ERAD. Fully folded clients dissociate and are transported to their sites of function (right). Misfolded proteins also disengage and display signals for degradation (left).

(B) In the absence of Slp1-Emp65 complex, newly synthesized proteins are subject to degradation. In this situation, fast folding proteins may fold quickly enough to avoid degradation while slow folding proteins (e.g., collagen) may be mostly degraded before molecules complete maturation.

like a general chaperone because the folding of membrane proteins, including those with large luminal domains like Gas1, is unaffected in its absence. Furthermore, the degradation of model ERAD substrates, molecules that can never fold, is accelerated in *slp1* and *emp65* mutants, a phenotype inconsistent with a role as a folding factor. Mutants of established folding factors, including Kar2, Scj1, and PDI, strongly impair degradation (Brodsky et al., 1999; Gillece et al., 1999; Kabani et al., 2003; Mehnert et al., 2015; Nishikawa et al., 2001).

This study reveals a new fundamental activity of protein homeostasis that adds a missing link between protein folding and quality control. With the available information, we propose the following model. The S-E complex, through the SUN-like domain of Slp1, binds to newly synthesized polypeptides soon after translocation (Figure 7A). They begin the folding process by attracting chaperones and folding catalysts. Sequestered, they are protected from ERAD pathways. Once a folded or partially folded state not vulnerable to degradation is reached, they dissociate to complete maturation in preparation to transport to their sites of function. The importance of the complex to proteostasis is the dramatic improvement on the efficiency of protein production compared to its absence. Without the S-E complex, the folding process competes with ERAD so only a fraction of molecules are able to fold fast enough to avoid degradation (Figure 7B).

STAR★METHODS

Detailed methods are provided in the online version of this paper and include the following:

- KEY RESOURCES TABLE
- CONTACT FOR REAGENT AND RESOURCES SHARING
- EXPERIMENTAL MODEL AND SUBJECT DETAILS
  - Yeast strains
  - Yeast cell culture
- METHOD DETAILS
  - Plasmid construction
  - Use of antibodies
  - ER-GFP^{fast} based genetic screen
  - Slp1 and Emp65 membrane topology prediction
  - Protein extraction and immunoblotting
  - Pulse-chase and immunoprecipitation assay
  - Analysis of unfolded protein response activity
  - Live cell imaging
  - Cycloheximide chase analysis
  - Co-immunoprecipitation assay
- QUANTIFICATION AND STATISTICAL ANALYSIS
  - Quantification in PC/IPA experiments
  - Quantification in immunoblotting
  - Statistical analysis

SUPPLEMENTAL INFORMATION

Supplemental Information includes seven figures and four tables and can be found with this article online at http://dx.doi.org/10.1016/j.cell.2017.08.036.

AUTHOR CONTRIBUTIONS

S.Z., C.X., K.E.L., and D.T.W.N. performed the molecular, genetic, and imaging analyses. S.Z., C.X., and K.E.L. performed the biochemical and quantitative analyses. C.X. and D.T.W.N. conceived and supervised the project. S.Z., C.X., K.E.L., and D.T.W.N. wrote the paper.

ACKNOWLEDGMENTS

We thank P. Walter (UCSF) for antibodies, S. Michaelis (Johns Hopkins Medical School) for her gift of pSM1083, and J. Brodsky (University of Pittsburgh)

for his gift of the ΔGppαF gene. We thank N. Bedford and Y. Liu for technical assistance. This work was supported by funds from the Temasek Trust. S.Z. is a recipient of The National University of Singapore Graduate Research Scholarship.

Received: April 5, 2017
Revised: July 6, 2017
Accepted: August 21, 2017
Published: September 14, 2017

REFERENCES

Ammerer, G., Hunter, C.P., Rothman, J.H., Saari, G.C., Valls, L.A., and Stevens, T.H. (1986). PEP4 gene of Saccharomyces cerevisiae encodes proteinase A, a vacuolar enzyme required for processing of vacuolar precursors. Mol. Cell. Biol. *6*, 2490–2499.

Araki, K., and Nagata, K. (2011). Protein folding and quality control in the ER. Cold Spring Harb. Perspect. Biol. *3*, a007526.

Aronson, D.E., Costantini, L.M., and Snapp, E.L. (2011). Superfolder GFP is fluorescent in oxidizing environments when targeted via the Sec translocon. Traffic *12*, 543–548.

Balchin, D., Hayer-Hartl, M., and Hartl, F.U. (2016). In vivo aspects of protein folding and quality control. Science *353*, aac4354.

Bhamidipati, A., Denic, V., Quan, E.M., and Weissman, J.S. (2005). Exploration of the topological requirements of ERAD identifies Yos9p as a lectin sensor of misfolded glycoproteins in the ER lumen. Mol. Cell *19*, 741–751.

Boudko, S.P., Engel, J., and Bächinger, H.P. (2012). The crucial role of trimerization domains in collagen folding. Int. J. Biochem. Cell Biol. *44*, 21–32.

Brodsky, J.L., Werner, E.D., Dubas, M.E., Goeckeler, J.L., Kruse, K.B., and McCracken, A.A. (1999). The requirement for molecular chaperones during endoplasmic reticulum-associated protein degradation demonstrates that protein export and import are mechanistically distinct. J. Biol. Chem. *274*, 3453–3460.

Buck, T.M., Plavchak, L., Roy, A., Donnelly, B.F., Kashlan, O.B., Kleyman, T.R., Subramanya, A.R., and Brodsky, J.L. (2013). The Lhs1/GRP170 chaperones facilitate the endoplasmic reticulum-associated degradation of the epithelial sodium channel. J. Biol. Chem. *288*, 18366–18380.

Buschhorn, B.A., Kostova, Z., Medicherla, B., and Wolf, D.H. (2004). A genome-wide screen identifies Yos9p as essential for ER-associated degradation of glycoproteins. FEBS Lett. *577*, 422–426.

Carvalho, P., Goder, V., and Rapoport, T.A. (2006). Distinct ubiquitin-ligase complexes define convergent pathways for the degradation of ER proteins. Cell *126*, 361–373.

Cherepanova, N., Shrimal, S., and Gilmore, R. (2016). N-linked glycosylation and homeostasis of the endoplasmic reticulum. Curr. Opin. Cell Biol. *41*, 57–65.

Christianson, J.C., and Ye, Y. (2014). Cleaning up in the endoplasmic reticulum: ubiquitin in charge. Nat. Struct. Mol. Biol. *21*, 325–335.

Christianson, J.C., Shaler, T.A., Tyler, R.E., and Kopito, R.R. (2008). OS-9 and GRP94 deliver mutant alpha1-antitrypsin to the Hrd1-SEL1L ubiquitin ligase complex for ERAD. Nat. Cell Biol. *10*, 272–282.

Clerc, S., Hirsch, C., Oggier, D.M., Deprez, P., Jakob, C., Sommer, T., and Aebi, M. (2009). Htm1 protein generates the N-glycan signal for glycoprotein degradation in the endoplasmic reticulum. J. Cell Biol. *184*, 159–172.

Copic, A., Dorrington, M., Pagant, S., Barry, J., Lee, M.C., Singh, I., Hartman, J.L., 4th, and Miller, E.A. (2009). Genomewide analysis reveals novel pathways affecting endoplasmic reticulum homeostasis, protein modification and quality control. Genetics *182*, 757–769.

Cox, J.S., and Walter, P. (1996). A novel mechanism for regulating activity of a transcription factor that controls the unfolded protein response. Cell *87*, 391–404.

Denic, V., Quan, E.M., and Weissman, J.S. (2006). A luminal surveillance complex that selects misfolded glycoproteins for ER-associated degradation. Cell *126*, 349–359.

Duttler, S., Pechmann, S., and Frydman, J. (2013). Principles of cotranslational ubiquitination and quality control at the ribosome. Mol. Cell *50*, 379–393.

Finger, A., Knop, M., and Wolf, D.H. (1993). Analysis of two mutated vacuolar proteins reveals a degradation pathway in the endoplasmic reticulum or a related compartment of yeast. Eur. J. Biochem. *218*, 565–574.

Fisher, A.C., and DeLisa, M.P. (2008). Laboratory evolution of fast-folding green fluorescent protein using secretory pathway quality control. PLoS ONE *3*, e2351.

Foresti, O., Rodriguez-Vaello, V., Funaya, C., and Carvalho, P. (2014). Quality control of inner nuclear membrane proteins by the Asi complex. Science *346*, 751–755.

Friederichs, J.M., Gardner, J.M., Smoyer, C.J., Whetstine, C.R., Gogol, M., Slaughter, B.D., and Jaspersen, S.L. (2012). Genetic analysis of Mps3 SUN domain mutants in Saccharomyces cerevisiae reveals an interaction with the SUN-like protein Slp1. G3 (Bethesda) *2*, 1703–1718.

Fujita, M., Yoko-O, T., and Jigami, Y. (2006). Inositol deacylation by Bst1p is required for the quality control of glycosylphosphatidylinositol-anchored proteins. Mol. Biol. Cell *17*, 834–850.

Gardner, R.G., Nelson, Z.W., and Gottschling, D.E. (2005). Degradation-mediated protein quality control in the nucleus. Cell *120*, 803–815.

Gauss, R., Kanehara, K., Carvalho, P., Ng, D.T., and Aebi, M. (2011). A complex of Pdi1p and the mannosidase Htm1p initiates clearance of unfolded glycoproteins from the endoplasmic reticulum. Mol. Cell *42*, 782–793.

Gillece, P., Luz, J.M., Lennarz, W.J., de La Cruz, F.J., and Römisch, K. (1999). Export of a cysteine-free misfolded secretory protein from the endoplasmic reticulum for degradation requires interaction with protein disulfide isomerase. J. Cell Biol. *147*, 1443–1456.

Gnann, A., Riordan, J.R., and Wolf, D.H. (2004). Cystic fibrosis transmembrane conductance regulator degradation depends on the lectins Htm1p/EDEM and the Cdc48 protein complex in yeast. Mol. Biol. Cell *15*, 4125–4135.

Heck, J.W., Cheung, S.K., and Hampton, R.Y. (2010). Cytoplasmic protein quality control degradation mediated by parallel actions of the E3 ubiquitin ligases Ubr1 and San1. Proc. Natl. Acad. Sci. USA *107*, 1106–1111.

Hein, M.Y., Hubner, N.C., Poser, I., Cox, J., Nagaraj, N., Toyoda, Y., Gak, I.A., Weisswange, I., Mansfeld, J., Buchholz, F., et al. (2015). A human interactome in three quantitative dimensions organized by stoichiometries and abundances. Cell *163*, 712–723.

Helenius, A., and Aebi, M. (2001). Intracellular functions of N-linked glycans. Science *291*, 2364–2369.

Helenius, A., and Aebi, M. (2004). Roles of N-linked glycans in the endoplasmic reticulum. Annu. Rev. Biochem. *73*, 1019–1049.

Hirayama, H., Fujita, M., Yoko-o, T., and Jigami, Y. (2008). O-mannosylation is required for degradation of the endoplasmic reticulum-associated degradation substrate Gas1*p via the ubiquitin/proteasome pathway in Saccharomyces cerevisiae. J. Biochem. *143*, 555–567.

Howell, G.R., Shindo, M., Murray, S., Gridley, T., Wilson, L.A., and Schimenti, J.C. (2007). Mutation of a ubiquitously expressed mouse transmembrane protein (Tapt1) causes specific skeletal homeotic transformations. Genetics *175*, 699–707.

Jonikas, M.C., Collins, S.R., Denic, V., Oh, E., Quan, E.M., Schmid, V., Weibezahn, J., Schwappach, B., Walter, P., Weissman, J.S., and Schuldiner, M. (2009). Comprehensive characterization of genes required for protein folding in the endoplasmic reticulum. Science *323*, 1693–1697.

Kabani, M., Kelley, S.S., Morrow, M.W., Montgomery, D.L., Sivendran, R., Rose, M.D., Gierasch, L.M., and Brodsky, J.L. (2003). Dependence of endoplasmic reticulum-associated degradation on the peptide binding domain and concentration of BiP. Mol. Biol. Cell *14*, 3437–3448.

Kanehara, K., Xie, W., and Ng, D.T. (2010). Modularity of the Hrd1 ERAD complex underlies its diverse client range. J. Cell Biol. *188*, 707–716.

Khmelinskii, A., Blaszczak, E., Pantazopoulou, M., Fischer, B., Omnus, D.J., Le Dez, G., Brossard, A., Gunnarsson, A., Barry, J.D., Meurer, M., et al. (2014). Protein quality control at the inner nuclear membrane. Nature *516*, 410–413.

Kim, W., Spear, E.D., and Ng, D.T. (2005). Yos9p detects and targets misfolded glycoproteins for ER-associated degradation. Mol. Cell *19*, 753–764.

Knop, M., Hauser, N., and Wolf, D.H. (1996). N-glycosylation affects endoplasmic reticulum degradation of a mutated derivative of carboxypeptidase yscY in yeast. Yeast *12*, 1229–1238.

Krogh, A., Larsson, B., von Heijne, G., and Sonnhammer, E.L. (2001). Predicting transmembrane protein topology with a hidden Markov model: application to complete genomes. J. Mol. Biol. *305*, 567–580.

Labbadia, J., and Morimoto, R.I. (2015). The biology of proteostasis in aging and disease. Annu. Rev. Biochem. *84*, 435–464.

Li, H.J., Xue, Y., Jia, D.J., Wang, T., Hi, D.Q., Liu, J., Cui, F., Xie, Q., Ye, D., and Yang, W.C. (2011). POD1 regulates pollen tube guidance in response to micropylar female signaling and acts in early embryo patterning in Arabidopsis. Plant Cell *23*, 3288–3302.

Loayza, D., and Michaelis, S. (1998). Role for the ubiquitin-proteasome system in the vacuolar degradation of Ste6p, the a-factor transporter in Saccharomyces cerevisiae. Mol. Cell. Biol. *18*, 779–789.

McCracken, A.A., and Brodsky, J.L. (1996). Assembly of ER-associated protein degradation in vitro: dependence on cytosol, calnexin, and ATP. J. Cell Biol. *132*, 291–298.

Mehnert, M., Sommermeyer, F., Berger, M., Kumar Lakshmipathy, S., Gauss, R., Aebi, M., Jarosch, E., and Sommer, T. (2015). The interplay of Hrd3 and the molecular chaperone system ensures efficient degradation of malfolded secretory proteins. Mol. Biol. Cell *26*, 185–194.

Molinari, M., Calanca, V., Galli, C., Lucca, P., and Paganetti, P. (2003). Role of EDEM in the release of misfolded glycoproteins from the calnexin cycle. Science *299*, 1397–1400.

Nakatsukasa, K., Huyer, G., Michaelis, S., and Brodsky, J.L. (2008). Dissecting the ER-associated degradation of a misfolded polytopic membrane protein. Cell *132*, 101–112.

Ng, D.T., and Walter, P. (1996). ER membrane protein complex required for nuclear fusion. J. Cell Biol. *132*, 499–509.

Ng, D.T., Brown, J.D., and Walter, P. (1996). Signal sequences specify the targeting route to the endoplasmic reticulum membrane. J. Cell Biol. *134*, 269–278.

Ng, D.T., Spear, E.D., and Walter, P. (2000). The unfolded protein response regulates multiple aspects of secretory and membrane protein biogenesis and endoplasmic reticulum quality control. J. Cell Biol. *150*, 77–88.

Nishikawa, S.I., Fewell, S.W., Kato, Y., Brodsky, J.L., and Endo, T. (2001). Molecular chaperones in the yeast endoplasmic reticulum maintain the solubility of proteins for retrotranslocation and degradation. J. Cell Biol. *153*, 1061–1070.

Nuoffer, C., Jenö, P., Conzelmann, A., and Riezman, H. (1991). Determinants for glycophospholipid anchoring of the Saccharomyces cerevisiae GAS1 protein to the plasma membrane. Mol. Cell. Biol. *11*, 27–37.

Oda, Y., Hosokawa, N., Wada, I., and Nagata, K. (2003). EDEM as an acceptor of terminally misfolded glycoproteins released from calnexin. Science *299*, 1394–1397.

Okuda-Shimizu, Y., and Hendershot, L.M. (2007). Characterization of an ERAD pathway for nonglycosylated BiP substrates, which require Herp. Mol. Cell *28*, 544–554.

Pfeiffer, A., Stephanowitz, H., Krause, E., Volkwein, C., Hirsch, C., Jarosch, E., and Sommer, T. (2016). A complex of Htm1 and the oxidoreductase Pdi1 accelerates degradation of misfolded glycoproteins. J. Biol. Chem. *291*, 12195–12207.

Prasad, R., Kawaguchi, S., and Ng, D.T. (2010). A nucleus-based quality control mechanism for cytosolic proteins. Mol. Biol. Cell *21*, 2117–2127.

Quan, E.M., Kamiya, Y., Kamiya, D., Denic, V., Weibezahn, J., Kato, K., and Weissman, J.S. (2008). Defining the glycan destruction signal for endoplasmic reticulum-associated degradation. Mol. Cell *32*, 870–877.

Rose, M.D., Misra, L.M., and Vogel, J.P. (1989). KAR2, a karyogamy gene, is the yeast homolog of the mammalian BiP/GRP78 gene. Cell *57*, 1211–1221.

Ruggiano, A., Foresti, O., and Carvalho, P. (2014). Quality control: ER-associated degradation: protein quality control and beyond. J. Cell Biol. *204*, 869–879.

Schneider, K., and Bertolotti, A. (2015). Surviving protein quality control catastrophes–from cells to organisms. J. Cell Sci. *128*, 3861–3869.

Silberstein, S., Schlenstedt, G., Silver, P.A., and Gilmore, R. (1998). A role for the DnaJ homologue Scj1p in protein folding in the yeast endoplasmic reticulum. J. Cell Biol. *143*, 921–933.

Sohaskey, M.L., Jiang, Y., Zhao, J.J., Mohr, A., Roemer, F., and Harland, R.M. (2010). Osteopotentia regulates osteoblast maturation, bone formation, and skeletal integrity in mice. J. Cell Biol. *189*, 511–525.

Sommer, T., and Jentsch, S. (1993). A protein translocation defect linked to ubiquitin conjugation at the endoplasmic reticulum. Nature *365*, 176–179.

Sosa, B.A., Rothballer, A., Kutay, U., and Schwartz, T.U. (2012). LINC complexes form by binding of three KASH peptides to domain interfaces of trimeric SUN proteins. Cell *149*, 1035–1047.

Spear, E.D., and Ng, D.T. (2003). Stress tolerance of misfolded carboxypeptidase Y requires maintenance of protein trafficking and degradative pathways. Mol. Biol. Cell *14*, 2756–2767.

Stolz, A., Besser, S., Hottmann, H., and Wolf, D.H. (2013). Previously unknown role for the ubiquitin ligase Ubr1 in endoplasmic reticulum-associated protein degradation. Proc. Natl. Acad. Sci. USA *110*, 15271–15276.

Szathmary, R., Bielmann, R., Nita-Lazar, M., Burda, P., and Jakob, C.A. (2005). Yos9 protein is essential for degradation of misfolded glycoproteins and may function as lectin in ERAD. Mol. Cell *19*, 765–775.

Thibault, G., Ismail, N., and Ng, D.T. (2011). The unfolded protein response supports cellular robustness as a broad-spectrum compensatory pathway. Proc. Natl. Acad. Sci. USA *108*, 20597–20602.

Thibault, G., Shui, G., Kim, W., McAlister, G.C., Ismail, N., Gygi, S.P., Wenk, M.R., and Ng, D.T. (2012). The membrane stress response buffers lethal effects of lipid disequilibrium by reprogramming the protein homeostasis network. Mol. Cell *48*, 16–27.

Vashist, S., and Ng, D.T. (2004). Misfolded proteins are sorted by a sequential checkpoint mechanism of ER quality control. J. Cell Biol. *165*, 41–52.

Vashist, S., Kim, W., Belden, W.J., Spear, E.D., Barlowe, C., and Ng, D.T. (2001). Distinct retrieval and retention mechanisms are required for the quality control of endoplasmic reticulum protein folding. J. Cell Biol. *155*, 355–368.

Vasnier, C., de Muyt, A., Zhang, L., Tessé, S., Kleckner, N.E., Zickler, D., and Espagne, E. (2014). Absence of SUN-domain protein Slp1 blocks karyogamy and switches meiotic recombination and synapsis from homologs to sister chromatids. Proc. Natl. Acad. Sci. USA *111*, E4015–E4023.

Wang, M., and Kaufman, R.J. (2016). Protein misfolding in the endoplasmic reticulum as a conduit to human disease. Nature *529*, 326–335.

Wang, S., Thibault, G., and Ng, D.T. (2011). Routing misfolded proteins through the multivesicular body (MVB) pathway protects against proteotoxicity. J. Biol. Chem. *286*, 29376–29387.

Ward, C.L., Omura, S., and Kopito, R.R. (1995). Degradation of CFTR by the ubiquitin-proteasome pathway. Cell *83*, 121–127.

Werner, E.D., Brodsky, J.L., and McCracken, A.A. (1996). Proteasome-dependent endoplasmic reticulum-associated protein degradation: an unconventional route to a familiar fate. Proc. Natl. Acad. Sci. USA *93*, 13797–13801.

Willer, M., Forte, G.M., and Stirling, C.J. (2008). Sec61p is required for ERAD-L: genetic dissection of the translocation and ERAD-L functions of Sec61P using novel derivatives of CPY. J. Biol. Chem. *283*, 33883–33888.

Xie, W., Kanehara, K., Sayeed, A., and Ng, D.T. (2009). Intrinsic conformational determinants signal protein misfolding to the Hrd1/Htm1 endoplasmic reticulum-associated degradation system. Mol. Biol. Cell *20*, 3317–3329.

Xu, C., and Ng, D.T. (2015). Glycosylation-directed quality control of protein folding. Nat. Rev. Mol. Cell Biol. *16*, 742–752.

Xu, C., Wang, S., Thibault, G., and Ng, D.T. (2013). Futile protein folding cycles in the ER are terminated by the unfolded protein O-mannosylation pathway. Science *340*, 978–981.

Youker, R.T., Walsh, P., Beilharz, T., Lithgow, T., and Brodsky, J.L. (2004). Distinct roles for the Hsp40 and Hsp90 molecular chaperones during cystic fibrosis transmembrane conductance regulator degradation in yeast. Mol. Biol. Cell *15*, 4787–4797.

STAR★METHODS

KEY RESOURCES TABLE

REAGENT or RESOURCE	SOURCE	IDENTIFIER
Antibodies		
Rabbit polyclonal anti-CPY	Thibault et al., 2012	N/A
Rabbit polyclonal anti-Gas1	Ng et al., 2000	N/A
Rabbit polyclonal anti-Htm1	Gauss et al., 2011	N/A
Rabbit polyclonal anti-Kar2	P. Walter (UCSF)	N/A
Rabbit polyclonal anti-Sec61	P. Walter (UCSF)	N/A
Mouse monoclonal anti-FLAG M2	Sigma-Aldrich	Cat# F1804-1MG; RRID: AB_262044
Anti-FLAG M2 Affinity Gel	Sigma-Aldrich	Cat# A2220-1ML; RRID: AB_10063035
Mouse monoclonal anti-HA.11 Clone 16B12	BioLegend	Cat# 901515; RRID: AB_2565334
Mouse monoclonal anti-GFP Clone 7.1 and 13.1	Roche	Cat# 11814460001; RRID: AB_390913
Mouse monoclonal anti-PGK1 Clone 22C5D8	Thermo Fisher Scientific	Cat# 459250; RRID: AB_2532235
Goat Anti-Rabbit IgG, IRDye 680LT Conjugated antibody	LI-COR Biosciences	Cat# 926-68021-0.5MG; RRID: AB_10706309
Goat Anti-Mouse IgG, IRDye 800CW Conjugated antibody	LI-COR Biosciences	Cat# 926-32210-0.5MG; RRID: AB_621842
Chemicals, Peptides, and Recombinant Proteins		
Endo H_f	New England Biolabs	Cat# P0703S
3 × FLAG peptide	Sigma-Aldrich	Cat# F4799-4MG
Protease Inhibitor Cocktail (PIC)	Sigma-Aldrich	Cat# P8215-5ML
Phenylmethanesulfonyl fluoride (PMSF)	Sigma-Aldrich	Cat# P7626-5G
EasyTag EXPRESS 35S	Perkin Elmer	Cat# NEG772014MC
o-Nitrophenyl β-D-galactopyranoside (ONPG)	Sigma-Aldrich	Cat# N1127-5G
Cycloheximide	Sigma-Aldrich	Cat# C1988-1G
Protein A-Sepharose	Sigma-Aldrich	Cat# P3391
Triton X-100	Sigma-Aldrich	Cat# T9284-500ML
Deposited Data		
Raw data	This paper	Mendeley data http://dx.doi.org/10.17632/y24zywhzzr.1
Experimental Models: Organisms/Strains		
Yeast strains used in this study are listed in Table S2	This study	N/A
Oligonucleotides		
Primers used in this study are listed in Table S3	This study	N/A
Recombinant DNA		
pRS316-p*TDH3*-ER-GFP^{fast}	Xu et al., 2013	pWX204
pRS314-p*UPRE-CYC1*-LACZ	Cox and Walter, 1996	pJC31
pRS315-p*PRC1*-CPY*-HA	Thibault et al., 2011	pGT69
pRS316-p*PEP4*-PrA*-HA	Xie et al., 2009	pKK117
pRS316-p*PRC1*-Htm1	Gauss et al., 2011	pKK225
pRS425 -p*YOS9*-Yos9-HA	Kim et al., 2005	pWK64
pRS316-p*PRC1*-abcd-CPY*-HA	Xie et al., 2009	pES149
pRS315-p*SEC61*-Sec61-2-HA	Vashist et al., 2001	pDN1002
pRS313-p*STE6*-Ste6*-HA	Loayza and Michaelis, 1998	pSM1083
pRS313-p*SLP1*-Slp1-HA	This study	pSZ37

(*Continued on next page*)

Continued

REAGENT or RESOURCE	SOURCE	IDENTIFIER
pRS314-p*SLP1*-Slp1-HA	This study	pSZ95
pRS315-p*PRC1*-CPY*-FLAG	This study	pSZ89
pRS315-p*PRC1*-abcd-CPY*-FLAG	This study	pSZ90
pRS315-p*PRC1*-DCPY*-HA	This study	pSZ151
pRS314-p*SLP1*-Slp1-FLAG	This study	pSZ96
pRS424-p*SLP1*-Slp1-FLAG	This study	pSZ98
pRS315-p*SLP1*-Slp1	This study	pSZ26
pRS314-p*EMP65*-Emp65	This study	pSZ27
pRS314-p*SLP1*-Slp1-ΔSLD-FLAG	This study	pSZ152
pRS424-p*SLP1*-Slp1-ΔSLD-FLAG	This study	pSZ159
pRS316-p*PRC1*-ΔGppαF-HA	Ng lab collection, modified from ΔGppαF expression vector (Werner et al., 1996)	pES17
Software and Algorithms		
TMHMM	Krogh et al., 2001	http://www.cbs.dtu.dk/services/TMHMM/
ImageQuant TL 8.1	GE Healthcare Life Sciences	http://www.gelifesciences.com/webapp/wcs/stores/servlet/catalog/en/GELifeSciences/products/AlternativeProductStructure_16011/29000605
Odyssey Infrared Imaging System 3.0	LI-COR Biosciences	https://www.licor.com/bio/products/imaging_systems/odyssey/
Prism 6.0	GraphPad Software	https://www.graphpad.com/
Summit 4.3	Beckman Coulter	http://www.beckman.com/coulter-flow-cytometry
Other		
4–15% Mini-PROTEAN TGX Stain-Free Gel	Bio-Rad	Cat# 4568086 and 4568084
0.2 μm Trans-Blot Turbo Midi Nitrocellulose Transfer Packs	Bio-Rad	Cat# 1704159
In-Fusion HD Cloning Kit	Clontech	Cat# 639649

CONTACT FOR REAGENT AND RESOURCES SHARING

Further information and requests for reagents may be directed to and will be fulfilled by the Lead Contact, Davis T.W. Ng (davisnglab@gmail.com).

EXPERIMENTAL MODEL AND SUBJECT DETAILS

Yeast strains

Yeast strains and their sources are listed in the Table S2.

Yeast cell culture

Yeast strains were cultured in standard synthetic complete (SC) media with specific components omitted as appropriate. Cell cultures were maintained at 30°C in experiments except in *cdc48-1* related experiments, in which cells were cultured at 30°C and shifted to 23°C prior to metabolic labeling.

METHOD DETAILS

Plasmid construction

Standard molecular cloning methods were used. All plasmid sequences (excluding standard vector sequences) were verified by DNA sequencing.

Slp1 and Emp65 expression vectors: A fragment containing the promoter, protein coding region and terminator of *SLP1* gene was amplified from yeast genomic DNA with SZO21 & SZO22 primers, digested with EagI and PstI, and inserted into the EagI-PstI site of pRS315 to generate pSZ26. Similarly, the *EMP65* gene was amplified from genomic DNA using SZO23 & SZO24. The PCR product was purified and digested with EagI-PstI and ligated to EagI-PstI digested pRS314 to generate pSZ27. To generate HA-tagged Slp1, *SLP1* promoter and protein coding sequences were amplified from pSZ26 with SZO21 and SZO63 and digested with EagI and NcoI. A fragment containing the HA epitope tag coding sequence and *ACT1* terminator was excised from pDN317 using NcoI and SalI (Ng et al., 1996). The fragments were ligated into EagI-SalI digested pRS313 to generate pSZ37. The pSZ37 insert was subcloned into pRS314 using SacI and XhoI to generate pSZ95. To generate FLAG-tagged Slp1(pSZ68), a fragment containing the FLAG coding sequence and *ACT1* terminator was amplified with SZO124 and SZO125 using pGT95 (pRS315-*OPI3*-FLAG-Actin terminator) as template and inserted into the NcoI-SalI sites of pSZ37. Using EagI and SalI, Slp1-FLAG was subcloned into pRS314 and pRS424 to generate pSZ96 and pSZ98, respectively. To generate the SUN-like domain deletion mutant Slp1-ΔSLD-FLAG (pSZ152), two fragments were amplified using SZO290-SZO292 and SZO291-SZO293 and pSZ96 as the template. Fragments were fused with EagI-NcoI digested pSZ96 using In-Fusion HD Cloning Kit. Using EagI and SalI, Slp1-ΔSLD-FLAG was subcloned into pRS424 to generate pSZ159.

CPY*-FLAG and abcd-CPY*-FLAG expression vectors: Using SZO151 and SZO152, CPY*-FLAG and abcd-CPY*-FLAG were amplified from pGT69 and pES149, respectively (Thibault et al., 2012; Xie et al., 2009). The fragments were digested with SacI and FseI and inserted into a pRS315 vector containing the *ACT1* terminator to generate pSZ89 and pSZ90.

DCPY* expression vector: DCPY* was generated by replacing the signal sequence of CPY* with the signal anchor sequence of DPAP B following the design of Stirling lab (Willer et al., 2008). The signal anchor sequence of DPAP B was amplified from pDN280 using SZO286 and SZO287 and digested with AscI and XmaI (Ng et al., 1996). CPY* without signal sequence was amplified with SZO288 and SZO289 using pGT69 as the template and digested with XmaI-FseI. Fragments were ligated into a pRS315 vector in which the coding sequence was under the control of a *PRC1* promoter and followed by an *ACT1* terminator to generate pSZ151.

Use of antibodies

Anti-HA monoclonal antibody was used to detect recombinant ERAD substrates (CPY*, Ste6*, PrA*, Sec61-2, abcd-CPY*, DCPY*, ΔGppαF) and Yos9-HA. Anti-FLAG monoclonal antibody was used to detect recombinant Slp1-FLAG, Slp1-ΔSLD-FLAG, CPY*-FLAG, and abcd-CPY*-FLAG. Specific polyclonal antisera were used for all other proteins.

ER-GFP^{fast} based genetic screen

The ER-GFP^{fast} expression vector was introduced into UPR-ON mutants that were identified in the previous study (Jonikas et al., 2009). Cells were grown to log phase and one OD_{600} unit of cells per strain was resuspended in ice-cold PBS and filtered (30 micron). Fluorescence intensity of 3×10^4 cells was determined by flow cytometry (CyAn ADP Analyzer, Beckman Coulter). In each experiment, the WT cells expressing an empty vector were used as a gating reference to eliminate signals from dead cells. To determine protein levels of the reporter, protein lysates were prepared in parallel using the same cultures and analyzed by quantitative immunoblotting as described below. The Pgk1 protein was probed as the loading reference for normalization.

Slp1 and Emp65 membrane topology prediction

The transmembrane domains and topology of Slp1 and Emp65 were predicted using the TMHMM algorithm (Krogh et al., 2001) (http://www.cbs.dtu.dk/services/TMHMM/). The predictions with the highest likelihood were followed. The first hydrophobic α-helix of Slp1 was suggested to be a signal peptide which is also supported by the previous study on the mouse ortholog of Slp1 (Sohaskey et al., 2010).

Protein extraction and immunoblotting

Cellular protein extracts were prepared as described previously (Wang et al., 2011). Two OD_{600} units of cells were harvested and resuspended in 1 mL of 10% trichloroacetic acid (TCA). After the addition of 0.8 mL of 0.5 mm zirconium beads, cells were lysed by mechanical agitation using a mini-bead beater (BioSpec Products) at 2 × 30 s pulses and a 5 min incubation on ice in between. Lysates were transferred into a fresh tube with remaining beads washed with 0.4 mL of 10% TCA and pooled. Extracts were pelleted by centrifugation for 10 min at 18,000 x*g* at 4°C. The pellet was resuspended in 80 μL of TCA resuspension buffer (100 mM Tris, pH 11.0, 3% SDS, 1 mM PMSF) and boiled for 10 min. The SDS insoluble fraction was pelleted by centrifugation for 10 min at 18,000 x*g* at 4°C. The SDS soluble fraction was separated by SDS-PAGE, and transferred to nitrocellulose membrane using the Trans-Blot Turbo Transfer System (Bio-RAD) with protocol set as: 2.5 A constant; up to 25 V; 7 min. After blocking and incubation with specific primary antibodies, washed membranes were incubated with anti-rabbit IRDye 680 and anti-mouse IRDye 800 secondary antibodies.

Pulse-chase and immunoprecipitation assay

Metabolic labeling and pulse-chase experiments were performed essentially as previously described with the following details and modifications (Ng et al., 2000). 3.0 OD_{600} units of cells grown at log phase were collected, resuspended in 900 μL of synthetic

complete or appropriate dropout media, and incubated at 30°C for 30 min unless otherwise indicated. Cells were pulse-labeled using 82.5 μCi of [^{35}S] methionine/cysteine (EasyTag EXPRESS ^{35}S, Perkin Elmer) for 5 or 10 min, as indicated in the text. The chase was initiated by adding unlabeled methionine/cysteine to a final concentration of 2 mM immediately after the pulse and terminated by adding TCA to 10% (w/v) at times indicated. Mechanical cell disruption and detergent extracts were performed as described above with 50 μL of TCA resuspension buffer per 1.0 OD_{600} units of cells used. Lysate volumes used for immunoprecipitation were normalized by TCA precipitable counts using a scintillation counter (LS6500, Beckman Coulter). 1.0 OD_{600} equivalent of cell lysate was incubated with 700 μL of IPS II solution (1% Triton X-100, 13.3 mM Tris, pH 7.5, 150 mM NaCl, 1.0 mM PMSF, 1.0 μL yeast protease inhibitor cocktail; Sigma-Aldrich) with appropriate antibody/antiserum at 4°C for 1 hr. Samples were centrifuged for 20 min 18,000 x*g* at 4°C. The supernatant was incubated with Protein A-Sepharose (Sigma-Aldrich) with nutation at 4°C for 2 hr. The tubes were then washed with 1.0 mL of IPS I solution (0.2% SDS, 1% Triton X-100, 20 mM Tris, pH 7.5, 150 mM NaCl) for 3 times and with 1.0 mL of PBS once. Immunoprecipitated proteins were eluted and separated by electrophoresis using 4%–15% SDS polyacrylamide gradient gels for most proteins or 8% SDS polyacrylamide gels for CPY and Gas1. Proteins were visualized and quantified by phosphorimager analysis (see Quantification and Statistical Analysis).

Analysis of unfolded protein response activity

Cells were transformed with pJC31, which contains the *UPRE-CYC1-LacZ* reporter gene. 6.0 OD_{600} units of cells were harvested in early log phase (OD_{600} < 0.4), washed once with 1 mL of Z buffer (125 mM sodium phosphate, pH 7, 10 mM KCl, 1 mM $MgSO_4$, 50 mM β-mercaptoethanol), and resuspended in 75 μL of Z buffer. 25 μL of the suspension was removed and mixed with 975 μL H_2O to determine the OD_{600} cell density. The reserved suspension was mixed with 50 μL $CHCl_3$ and 20 μL 0.1% SDS and vortexed vigorously for 20 s. 700 μL of Z buffer containing 2.0 mg/mL ONPG (*o*-Nitrophenyl β-D-galactopyranoside; Sigma-Aldrich) was added and the mixture was incubated at 30°C for 5-10 min. The reaction was quenched with 500 μL 1 M Na_2CO_3 at appropriate time point. Cells and debris were removed by centrifugation and OD_{420} and OD_{550} values of the supernatant were measured. β-galactosidase activity was calculated as follows: Miller units = $1000 \times (OD_{420} - 1.75 \times OD_{550})/(2t \times OD_{600})$ where t = time in minutes.

Live cell imaging

Cells expressing ER-GFP^{fast} were grown to log phase at 30°C and collected by brief centrifugation and were resuspended in PBS. Live cell imaging was performed on Zeiss Axiovert microscope with a 100 × 1.4 NA oil Plan-Apochromat objective (Carl Zeiss MicroImaging, Inc). GFP fluorescence was excited with a 488 nm laser and was detected with detector gain been set to 535.

Cycloheximide chase analysis

2.0 OD_{600} units of exponentially growing cells were collected and resuspended in 900 μL of synthetic complete media and incubated at 30°C for 30 min. The chase was initiated by adding the translation inhibitor cycloheximide to a final concentration of 200 μg/mL. Each time of chase was terminated by adding TCA to the culture at a final concentration of 10%. Cell extracts were prepared and analyzed by quantitative immunoblotting as described above.

Co-immunoprecipitation assay

Co-immunoprecipitation experiments were performed as previously described with the following modifications (Denic et al., 2006). 60-100 OD_{600} units of cells were harvested by centrifugation and resuspended in 500 μL of HEPES buffer (50 mM HEPES-KOH, pH 6.8, 150 mM KOAc, 2.0 mM $Mg(OAc)_2$, 1.0 mM $CaCl_2$, 15% glycerol) containing 0.1% Triton X-100, protease inhibitor cocktail (Sigma-Aldrich) and 2 mM of PMSF. Cells were disrupted by bead-beating by vortexing at maximum speed for 1 min five times with incubation on ice for 2 min between intervals. Cell lysates were clarified by two rounds of centrifugation at 1,000 x*g*. An equal volume of HEPES buffer containing 1.9% Triton X-100 was added resulting in a final concentration of 1%. After nutating for 1 hr at 4°C, the insoluble fraction was removed by centrifugation at 50,000 x*g* for 30 min. 40 μL of M2 anti-FLAG resin (Sigma-Aldrich) was added to the lysate and incubated at 4°C for 3 hr. After washing with HEPES buffer containing 1% Triton X-100 for four times, the complexes were eluted with triple-FLAG peptide at a concentration of 0.5 mg/mL and analyzed by SDS-PAGE and immunoblotting.

QUANTIFICATION AND STATISTICAL ANALYSIS

Quantification in PC/IPA experiments

In PC/IPA experiments, labeled proteins separated by SDS-PAGE were visualized using an Amersham Typhoon 9200 phosphorimager and quantified using ImageQuantTM TL software (GE healthcare Life Sciences). WT CPY biogenesis and stability were quantified by summing p1 (ER), p2 (Golgi), and m (vacuolar) forms for each time point. To correct for the loss of the pro domain (containing one of six methionine residues in proCPY) when p2 CPY is proteolytically processed to mCPY in the vacuole, signal values for mCPY are multiplied by 1.2. The data, without correction, are presented in Figures S3B and S3C.

Quantification in immunoblotting

In quantitative immunoblots, proteins of interest were visualized and quantified with Odyssey infrared imaging system (LI-COR Biosciences). The background correction settings were as follows. Background method: average. Border width: 3. Segment for

average and median method: top/bottom. Unrelated proteins indicated (Pgk1 and Sec61) were used as loading controls for signal normalization.

Statistical analysis

For experiments with quantification, a minimum of three independent replicates were performed unless otherwise indicated. The exact number of replicates is listed in the Table S4. Error bars in data plots represent the standard error of the mean (±SEM). When error bars are not visible, they are smaller than the symbols, except for Figures S4B and S5B, which present the average of two replicates and no error bar is shown. Two-tailed, unpaired Student's t test was performed to evaluate the statistical significance of observed differences between two strains using Prism software. Significance level is plotted ($p \geq 0.05$ not significant (n.s.), $^{*}p < 0.05$, $^{**}p < 0.01$, $^{***}p < 0.001$).

Cell

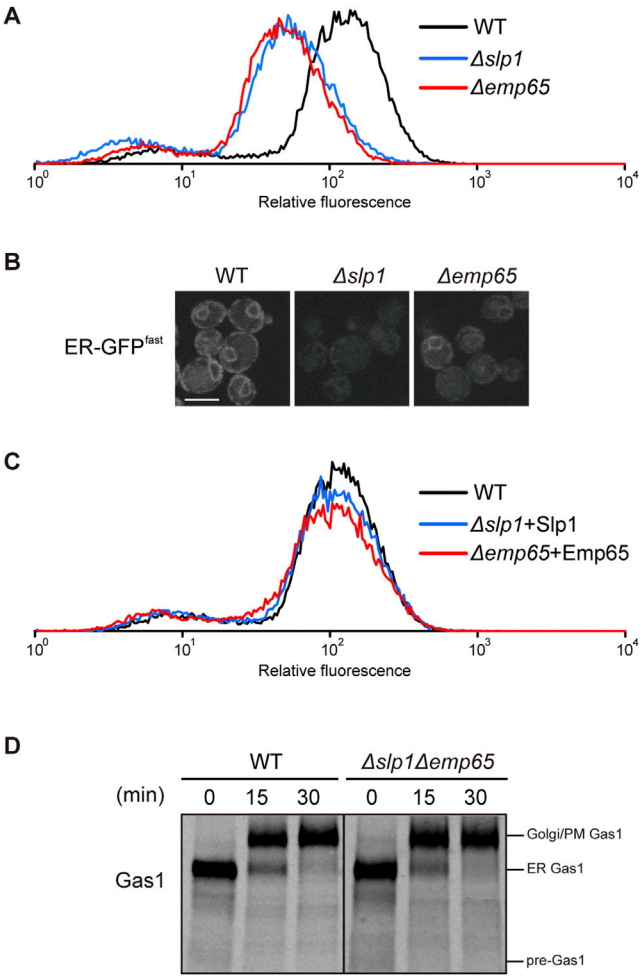


Figure S1. A Screen for Mutants with Disrupted ER Function Identifies *SLP1* and *EMP65*, Related to Figure 1

(A) Fluorescence activity of ER-GFP^{fast} in the WT, *Δslp1*, and *Δemp65* cells determined by flow cytometry.

(B) Fluorescence microscopy of ER-GFP^{fast} in WT, *Δslp1,* and *Δemp65* cells. Scale bar, 5 μm.

(C) *SLP1* or *EMP65* containing centromeric plasmids transformed into *Δslp1* and *Δemp65* cells, respectively. Plot represents the relative fluorescence activity of ER-GFP^{fast} in complemented strains.

(D) Maturation of Gas1 monitored by pulse-chase/immunoprecipitation assay (PC/IPA) in WT and *Δslp1Δemp65* double mutant cells as described in Figure 1C.

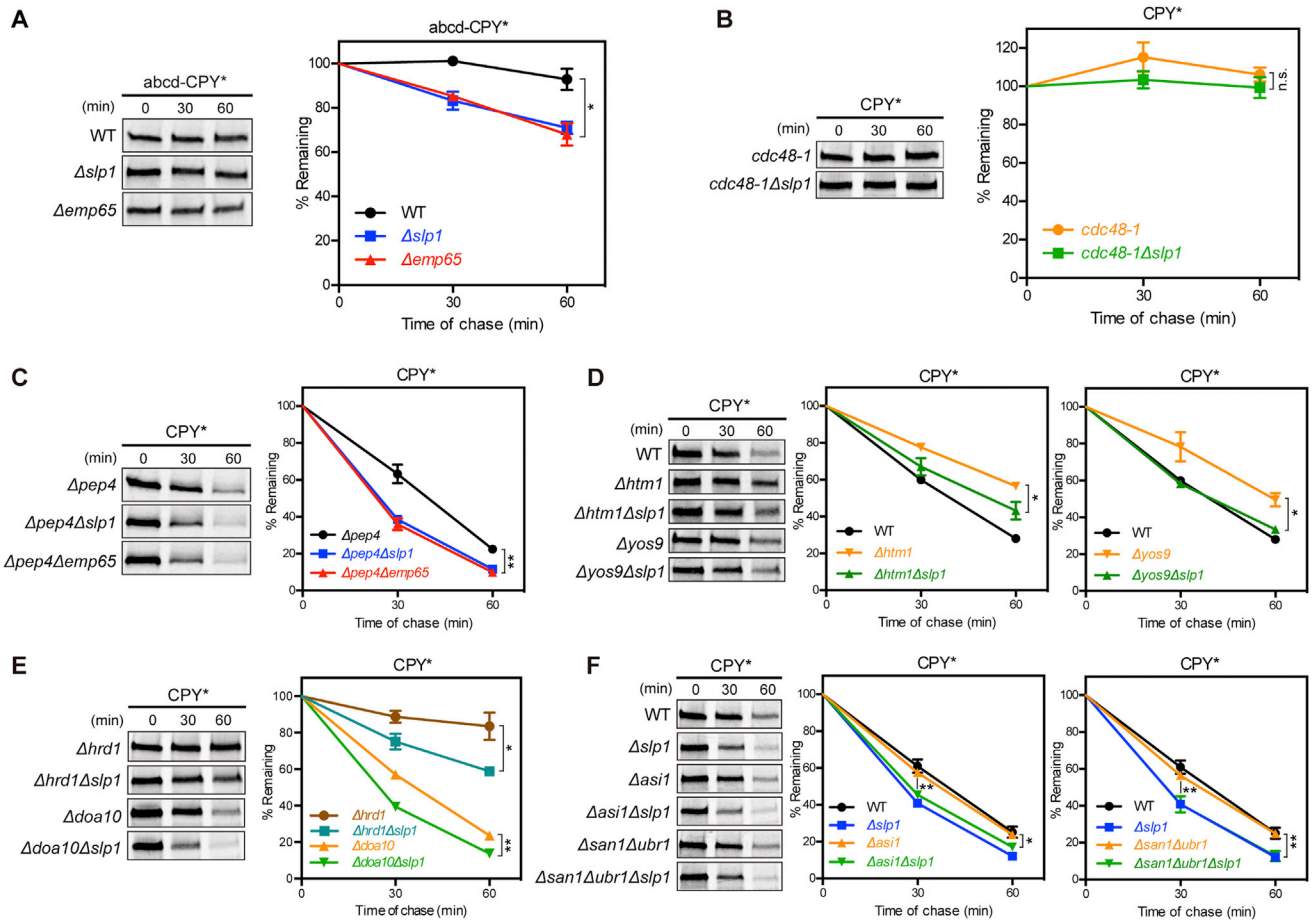


Figure S2. ERAD Pathways, but Not Vacuolar Proteases, Are Responsible for Enhanced Degradation in Cells Lacking the S-E Complex, Related to Figure 2

(A) Degradation of abcd-CPY*, a non-glycosylated variant of CPY*, was analyzed as described in Figure 2A.

(B) Turnover of CPY* was assayed by PC/IPA in *cdc48-1* and *cdc48-1Δslp1* cells at 23°C.

(C) CPY* degradation was analyzed by PC/IPA in *Δpep4*, *Δpep4Δslp1* and *Δpep4Δemp65* cells as described in Figure 2A.

(D) CPY* degradation was monitored by PC/IPA experiment in WT, *Δhtm1*, *Δhtm1Δslp1, Δyos9*, and *Δyos9Δslp1* cells as described in Figure 2A.

(E) Turnover of CPY* was assayed by PC/IPA in *Δhrd1*, *Δhrd1Δslp1*, *Δdoa10* and *Δdoa10Δslp1* cells as described in Figure 2A.

(F) CPY* degradation was analyzed by PC/IPA in WT, *Δslp1*, *Δasi1*, *Δasi1Δslp1*, *Δsan1Δubr1* and *Δsan1Δubr1Δslp1* cells as described in Figure 2A. Data represent mean ± SEM.

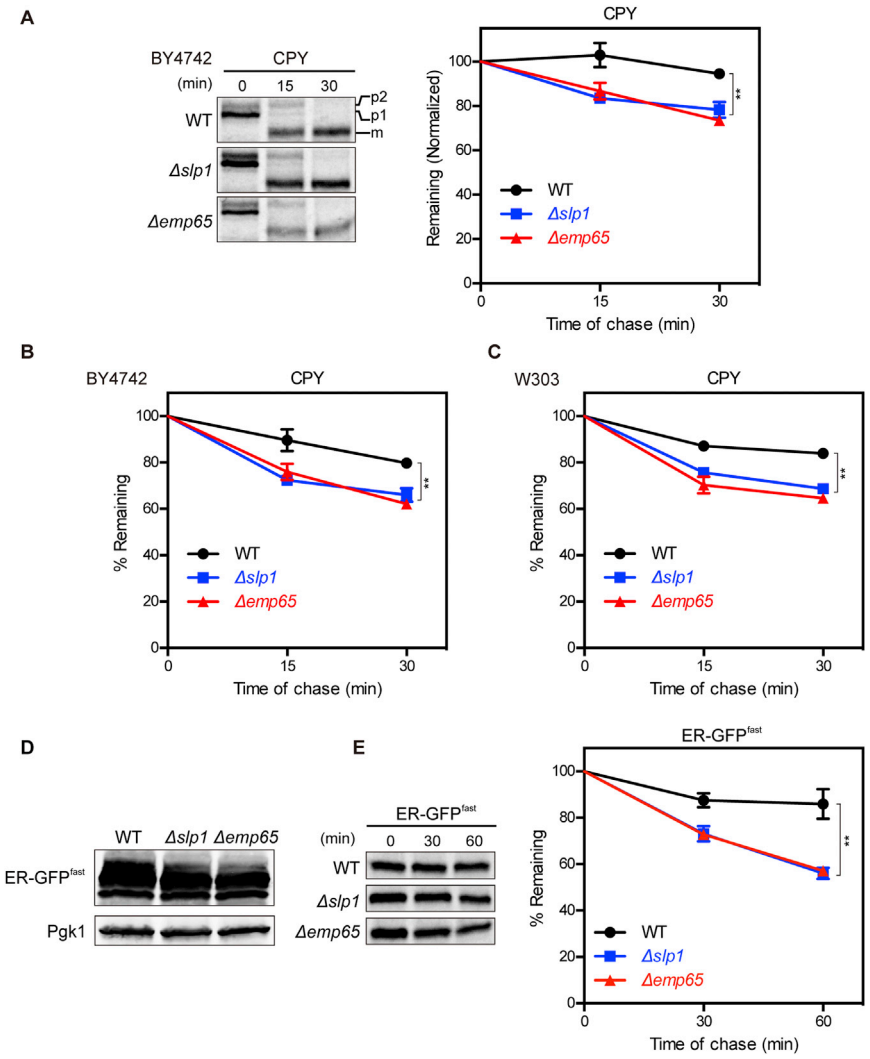


Figure S3. Promiscuous Degradation of Newly Synthesized Proteins in *Δslp1* and *Δemp65* Cells Is Independent of Strain Background and Is Not Restricted to Yeast Endogenous Proteins, Related to Figure 3

(A) The processing of endogenous CPY was analyzed in WT, *Δslp1* and *Δemp65* cells (BY4742 strain background). Cells were pulse-labeled for 5 min and chase for times indicated. CPY was immunoprecipitated using anti-CPY antiserum. The data used in the plot indicate normalized values as described in the STAR Methods.

(B) Plot using uncorrected data shown Figure S3A (BY4742).

(C) Plot using uncorrected data shown in Figure 3D (W303).

(D) Cell extracts were prepared from WT, *Δslp1*, and *Δemp65* cells expressing ER-GFP^{fast} and analyzed by immunoblotting using anti-GFP antibody. Pgk1 was probed as a loading control.

(E) WT, *Δslp1*, and *Δemp65* cells expressing ER-GFP^{fast} were pulse-labeled for 10 min with [^{35}S]Met/Cys and chased for the times indicated followed by immunoprecipitation of protein lysates using anti-GFP antibody. Data represent mean ± SEM.

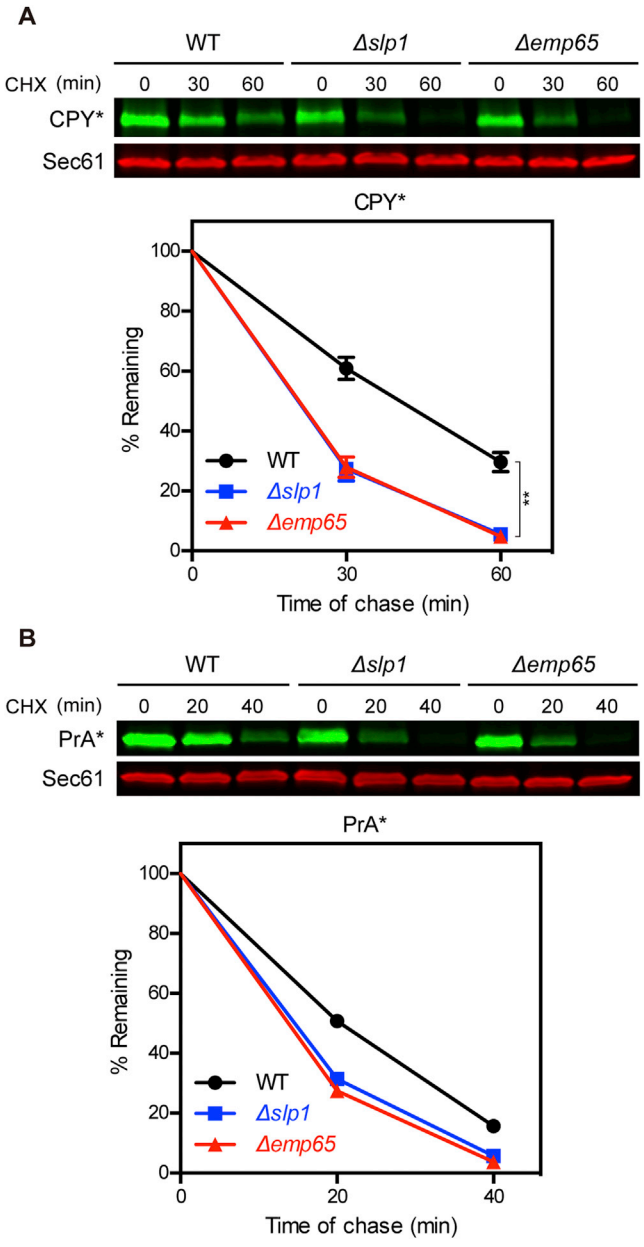


Figure S4. Steady-State Degradation of Soluble ERAD Substrates Is Enhanced in *Δslp1* and *Δemp65* Cells, Related to Figure 3

(A and B) The stability of CPY* or PrA* at steady state was assayed by cycloheximide chase. Logarithmically growing cells in liquid culture were treated with 200 μg/ml of cycloheximide and chased for times indicated. Cell extracts were separated by SDS-PAGE and analyzed by quantitative immunoblotting. In (A), data represent mean ± SEM. The quantification of (B) represents the average of two independent experiments.

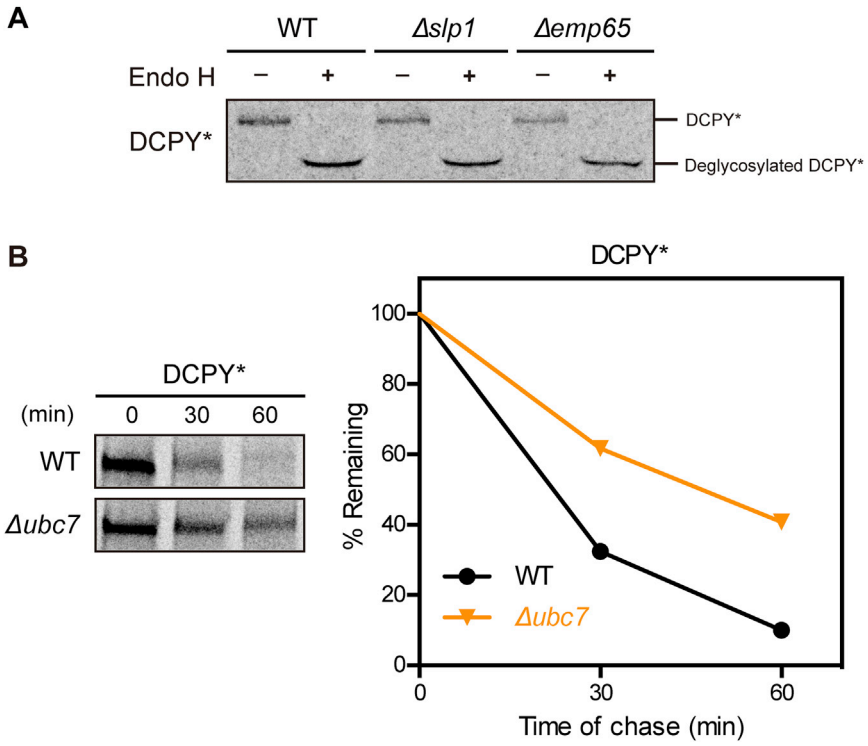


Figure S5. DCPY* Is a Luminally Oriented Transmembrane ERAD Substrate, Related to Figure 4

(A) WT, *Δslp1* and *Δemp65* cells expressing DCPY* were pulse-labeled for 5 min. DCPY* was immunoprecipitated using anti-HA antibody. The samples were split and treated with endoglycosidase H (+) or mock treated (-). After incubation at 30°C, proteins were separated by SDS-PAGE and visualized using a phosphorimager. The positions of DCPY* and deglycosylated DCPY* are indicated.

(B) Degradation of DCPY* was analyzed by PC/IPA experiments in WT and *Δubc7* cells. The quantification represents the average of two independent experiments.

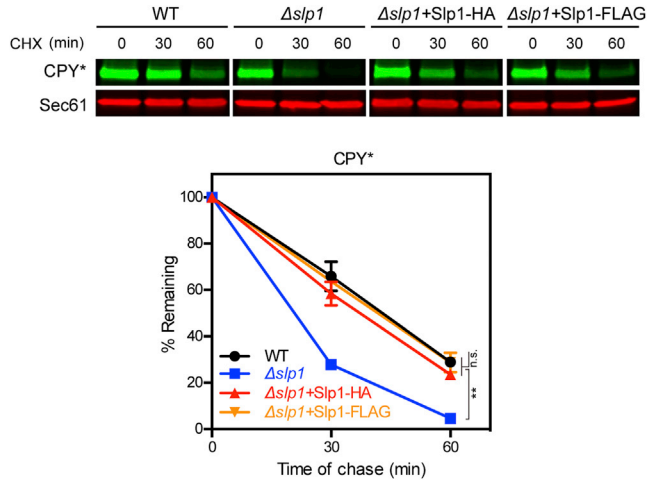


Figure S6. Epitope-Tagged Slp1 Is Functional, Related to Figure 5

Slp1-HA and Slp1-FLAG were expressed from centromeric plasmids under the control of the *SLP1* promoter. CPY* degradation was analyzed by cycloheximide chase assay and visualized by quantitative immunoblots (upper panel). Slp1-HA and Slp1-FLAG each fully reversed enhanced CPY* degradation in the *Δslp1* cells (lower panel). Data represent mean ± SEM.

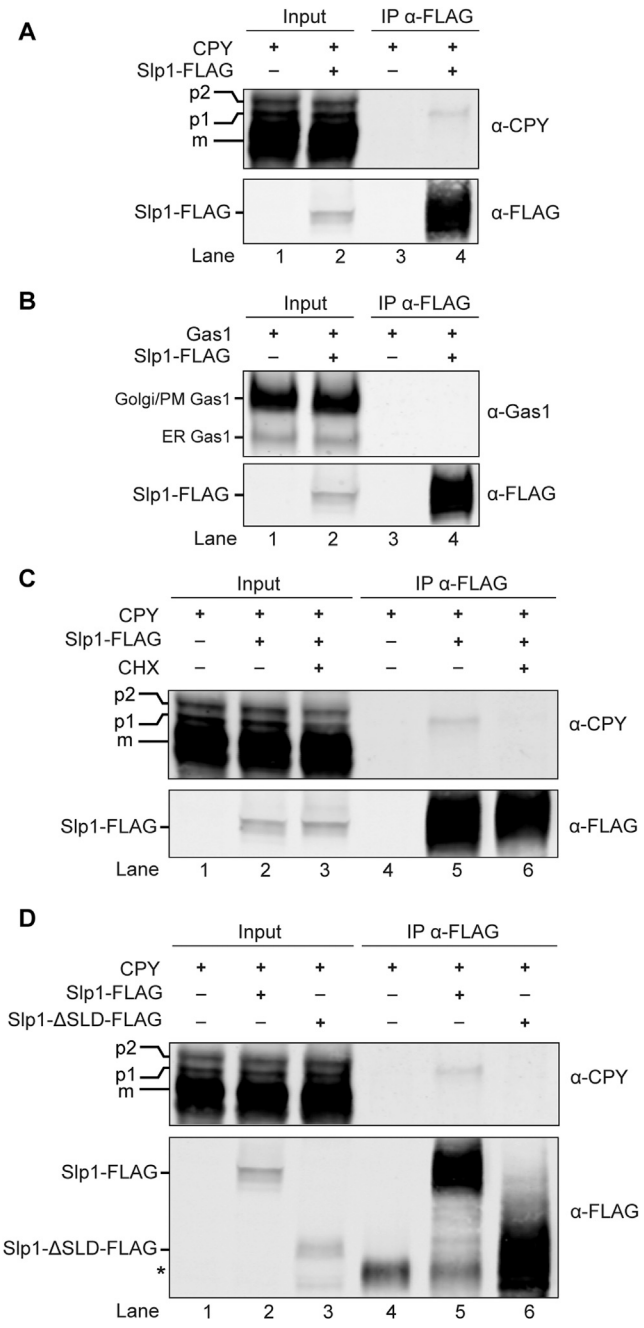


Figure S7. Slp1 Specifically Binds to Unfolded Soluble Proteins in the ER, Related to Figure 5

(A) Immunoprecipitation experiment as in Figure 5B, 5% of the total lysates were loaded as input.

(B) Experiment as in Figure 5C, 5% of the total lysates were loaded as input.

(C) Experiment as in Figure 5E, 5% of the total lysates were loaded as input.

(D) Experiment as in Figure 5G, 5% of the total lysates were loaded as input.